DOI: 10.1002/adsc.200600431

Conceptual, Qualitative, and Quantitative Theories of 1,3-Dipolar and Diels–Alder Cycloadditions Used in Synthesis

Daniel H. Ess,[a] Gavin O. Jones,[a] and K. N. Houk[a,*]

[a] Department of Chemistry and Biochemistry, University of California, Los Angeles, California 90095-1569, USA
Fax: (+1)-310-206-1843; e-mail: houk@chem.ucla.edu

Received: August 23, 2006; Accepted: September 27, 2006

Abstract: The application and performance of conceptual and qualitative theories and quantitative quantum mechanical methods to the study of mechanism, reactivity, and selectivity of 1,3-dipolar and Diels–Alder cycloadditions are reviewed. This review emphasizes the application of conceptual density functional theory (DFT) for predicting reactivity and regioselectivity, and highly accurate quantum mechanical methods for predicting barrier heights and reaction energetics. Applications of computations to solvation effects, metal and organocatalysis, are also described.

Keywords: conceptual density functional theory; configuration mixing; Diels–Alder cycloadditions; 1,3-dipolar cycloadditions; frontier molecular orbital theory; hard and soft acid and base theory

1 Introduction

Theory has played a significant role in the use of cycloadditions in synthesis.[1] Frontier molecular orbital (FMO) theory is a practical working tool for synthetic chemists and probably will be for some time. However, with the advent of density functional theory (DFT) and the ability to carry out experimentally accurate calculations, new conceptual models and quantitative quantum mechanical methods have been applied to a variety of 1,3-dipolar and Diels–Alder cycloadditions.[2] These recent qualitative and quantitative analyses have provided rich insights into reactivity, selectivity, and mechanisms of cycloadditions.

This article reviews the application and performance of conceptual theories and quantitative methods toward issues such as reactivity and selectivity.[3] This review is composed of three parts. Section 2 introduces FMO theory and its wide application, identifies evident shortcomings of this qualitative theory, and highlights popular conceptual and qualitative models for cycloadditions with emphasis on the emerging application of conceptual DFT for predicting reactivity and regioselectivity in Section 2.2. In Section 3, the most reliable quantitative thermochemistries for Diels–Alder and 1,3-dipolar cycloadditions are reviewed. Benchmark investigations of cycloadditions that provide critical evaluations of the accuracy and precision of *ab initio* and DFT methods are reviewed. Section 4 reviews recent applications of computations toward solvation effects, metal catalysis, and organocatalysis in cycloadditions.

2 Qualitative Treatments

2.1 Frontier Molecular Orbital (FMO) Theory

Frontier molecular orbital theory has proven to be a powerful conceptual framework to understand reactivities and selectivities in many types of reactions.[4] Developed by Fukui, it employs perturbation theory

Daniel Ess was born in 1981 in California and grew up in Utah. He attended a vocational college in his teenage years and then graduated from Brigham Young University in 2000. As a graduate student in K. N. Houk's lab, he is actively investigating cycloadditions using highly accurate quantum mechanical methods and developing new reactivity models. He is an IGERT-NSF fellow at UCLA.

Gavin Jones was born in St. Thomas, Jamaica in 1981. Since 2003 he has been a graduate student in the Department of Chemistry and Biochemistry at UCLA where he has been working in the labs of Prof. Kendall N. Houk's group at UCLA. His thesis work focuses on computational investigations of substituent effects on the rates of pericyclic reactions.

Kendall N. Houk obtained his Ph.D. in 1968 under the direction of R. B. Woodward. He has held faculty positions at Louisiana State University, University of Pittsburgh, and UCLA since 1985. He received the American Chemical Society James Flack Norris Award in Physical Organic Chemistry and the Award for Computers in Chemical and Pharmaceutical Research. He is a fellow of the American Academy of Arts and Sciences, the World Association of Theoretical and Computational Chemists, and the International Academy of Quantum Molecular Science. Among his major interests are the experimental and theoretical investigations of cycloaddition chemistry.

and emphasizes the interactions of the highest occupied molecular orbital (HOMO) and the lowest unoccupied molecular orbital (LUMO), the "frontier orbitals," of reacting molecules. Orbitals that are closest in energy interact most strongly. Smaller HOMO–LUMO gaps lead to lower activation barriers for reactions. Stabilization is also related to the square of the total overlap between the HOMO of one component and the LUMO of the other.

The prediction of reactivity, and regioselectivity patterns in pericyclic reactions is the most common application of FMO theory.[4a–f] The examples in Figure 1 show the normal electron demand Diels–Alder reaction between methyl acrylate and 1,3-dimethoxybuta-1,3-diene (Figure 1a and b) and the [2+2] cycloaddition of ethylene (Figure 1c), illustrate the principles of FMO theory which may be applied to other cycloadditions.[5]

For the reaction of dimethoxybutadiene with methyl acrylate, the signs of the lobes on the termini of the HOMO of the diene match those on the LUMO of the dienophile; the same is true for the combination involving the LUMO of the diene and the HOMO of the dienophile (Figure 1b). Both of these cycloadditions are allowed. In contrast, the cycloaddition of ethylene is forbidden because of the lack of stabilizing interaction between the LUMO and HOMO of the ethylene molecules (Figure 1c).

The interaction of the HOMO of 1,3-dimethoxybutadiene and the LUMO of the methyl acrylate has a gap of 11 eV; this separation, being smaller than that of the other combination provides the main stabilization of the transition state. Consequently, regioselectivity in pericyclic reactions is related to better overlap between the lobes of the orbitals that possess the largest orbital coefficients. In the FMOs of this example, the substituents polarize the frontier orbitals of the diene and the dienophile so that the β carbon of the LUMO of the dienophile and C-4 of the HOMO of the diene have the largest orbital coefficients. In the transition state, the degree of bond formation between these atoms is largest. The bond formed between C-4 and the β carbon occurs before the bond formed by C-1 of the diene and the α carbon of the dienophile. This leads to a degree of asymmetry of the transition state that is dependent on the ability of

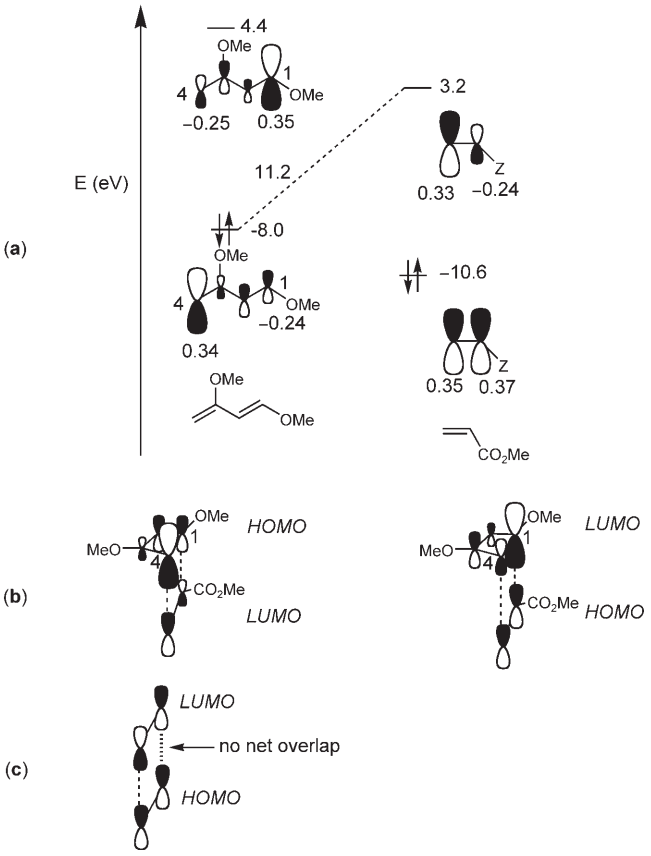

Figure 1. (**a**) Frontier molecular orbitals and (**b**) primary orbital interactions for the reaction of 1,3-dimethoxy-1,3-butadiene with methyl acrylate. Orbital energies by HF/6-31G(d) are shown in eV and orbital coefficients on reacting atoms are shown below the orbitals of the reactants. (**c**) Primary orbital interactions in the pericyclic reaction of two ethylene molecules.

the substituents on the diene and dienophile to stabilize the charge that develops on each reactant at the transition state.

For the vast majority of reactions considered, FMO theory predicts reactivities and selectivities that are in agreement with experiment. This, coupled with the ease of application of the method, has resulted in the widespread treatment of pericyclic reactions by FMO theory since being developed. Despite the popularity of FMO theory, however, a number of deficiencies have been identified, mainly due to the lack of quantitative significance of these FMO interactions. Alston and co-workers have pointed out that the interaction of secondary orbitals may at times outweigh the primary interactions that were shown in Figure 1.[6] These secondary orbital interactions involve orbitals that are not directly involved in the formation of new bonds, for example, the interaction of internal diene carbons with the electron-withdrawing substituent of the dienophile. Because the theory is only approximate, FMO theory does not always adequately account for the relative directing effects of substituents in polysubstituted dienes, or the influence of one type of substituent in different diene positions.[7] Singleton and co-workers have recently noted that because FMO theory utilizes ground state electronic configurations to describe reactivity, it may predict incorrect trends if the electronic configuration changes significantly near the transition state of the reaction.[8]

Recently, Spino et al. noted that in Diels–Alder cycloadditions involving electron-deficient dienes, FMO theory effectively predicts reactivity patterns of different dienophiles in normal electron demand reactions but failed to predict reactivities in inverse electron demand reactions.[9] In inverse electron demand reactions, unsymmetrical dienophiles are more reactive than symmetrical dienophiles. This is unaffected by the HOMO energies of dienophiles, and, therefore, the relative sizes of the $HOMO_{dienophile}$–$LUMO_{diene}$ gaps are not indicative of reactivities in these reactions. They suggest that the sizes of the orbital coefficients of the reactants are better indicators of the reactivity patterns in these types of reactions.

FMO theory remains a good qualitative guide to reactivity and selectivity, but because it is not a complete theory, it is not quantifiable.

2.2 Conceptual Density Functional Theory (DFT) and Hard and Soft Acid and Base (HSAB) Theory

The popularity and success of density functional theory (DFT) has stimulated many groups to use Hard and Soft Acid and Base (HSAB) theory, formulated with DFT, as a qualitative and quantitative treatment to predict reactivity based upon ground state properties (density) in a similar fashion to FMO theory.[10] This is an important development, since DFT is based upon the idea that electron densities can quantitatively account for energies and all properties; that is, molecular orbitals are unnecessary to explain chemistry. Conceptual DFT uses no orbitals, although it can be shown to be quantitatively related to FMO ideas. This theory has been applied to carbene reactivity,[11] S_N2 reactions,[12] enolate formation,[13] tautomerizations,[14] metal complexes,[15] enzymatic catalysis,[16] and many other organic reactions including cycloadditions.[17]

HSAB theory began as a classification of Lewis acids and bases as hard or soft based on properties such as ionization energies and polarizabilities.[18] Soft bases (electron donors) have high polarizability, low electronegativity, and low ionization energies. Hard bases have opposite properties, such as high negative charge, low polarizability and relatively high ionization energies. Soft acids (electron acceptors) have low charge, large size, are polarizable, and have high electron affinities. Hard acids are the opposite with large

positive charge, low polarizability, and low electron affinities. A basic axiom of HSAB theory is that soft-soft or hard-hard interactions are best. Soft-soft interactions are best described as charge transfer and arise from orbital interactions. Hard-hard interactions are mainly electrostatic in nature.[18c,d]

Over the last decade, Parr and others have laid a theoretical foundation of HSAB theory based on DFT principles.[2,10,19] The essence of HSAB, as formulated within DFT, is the transformation of the above definitions of hard and soft into chemical potential, μ, hardness, η, and softness, S. The interaction energy, ΔE_{int}, between two molecules is composed of two terms, a soft-soft (charge transfer or covalent) interaction term, ΔE_{υ}, and a hard-hard (electron reorganization or electrostatic) interaction term, ΔE_{μ}.[20] These interaction terms are defined in terms of chemical potential, μ, and softness, S. The chemical potential μ, is the tendency of electrons to be transferred to or from a molecule to another molecule. It is defined as the partial derivative of the energy with respect to the charge, that is the change in energy of a system with the change in the number of electrons at a constant nuclear geometry. This partial derivative is often approximated as the ionization potential (IP) plus the electron affinity (EA) divided by $^1/_2$. When an IP is high (it is difficult to remove an electron), and the EA is high (easy to add an electron) the chemical potential, μ, is a large number. The negative of the chemical potential is the absolute electronegativity, χ. When two systems have different chemical potentials (different electronegativities), electron density flows from a high to low chemical potential (or from low electronegativity to high electronegativity) until equilibrium is reached and a new chemical potential is obtained for the composite system.[18]

The hardness value, η, (often expressed as its inverse, the softness value, S) defines how the chemical potential changes with change in electron number. The hardness is the second partial derivative of the chemical potential, and is often approximated to be (IP−EA)/2.[18] The difference between the IP and EA is related to the polarizability or hardness of a molecule. In orbital terms, this would be the HOMO–LUMO gap. A small HOMO–LUMO gap relates to high polarizability, resulting from mixing of filled with vacant orbitals and stabilization upon perturbation. Molecules with a large IP−EA or HOMO–LUMO gap, undergo little or no polarization upon perturbation. The molecule is hard, and resistant to change.

An electronegativity difference (or chemical potential difference) promotes the interaction of two systems by change or electron transfer, while the hardness resists the charge transfer interaction (Figure 2).[10,18,19] The ionization energy and electron affinity are properties of a molecule that are actually independent of orbitals, even though the connection

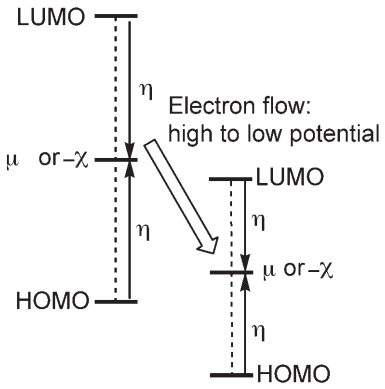

Figure 2. Qualitative diagram depicting the HOMO–LUMO gap, chemical potential, hardness, and electron flow between two species based on a difference in chemical potentials.

between HSAB theory and FMO theory is often made through Koopmans' theorem that equates the negatives of the HOMO and LUMO energies to the IP and EA, respectively.[10]

The chemical potential and hardness outlined above are molecular or global DFT descriptors. These provide an idea of reactivity. Application to the understanding of regioselectivity involves the Fukui function *f(r)*, which gives information equivalent to local softness.[19,21] The Fukui function, *f(r)*, is defined as the change in electron density at a given atomic site with the change in number of electrons at a constant nuclear geometry. An atomic site with a large Fukui function value is soft, while a site with a small Fukui function is hard.[20] Three Fukui functions exist that involve interactions with electrophiles or positive charge, $f^-(r)$, with nucleophiles or negative charge, $f^+(r)$, or a combination of the two as in radical or pericyclic reactions. The $f^-(r)$ and $f^+(r)$ are qualitatively related to the shapes of the HOMO and LUMO, respectively.[19e] From a practical standpoint, the values of these functions are approximated by computation of charges at each atom in the cation, anion, and neutral states:[2,10]

$$f^-(r \approx q(N)-q(N-1)=q(\text{Neutral})-q(\text{Cation})$$

electrophilic attack (acts as an nucleophile);

$$f^+(r) \approx q(N+1)-q(N)=q(\text{Anion})-q(\text{Neutral})$$

nucleophilic attack (acts as an electrophile);

$$f^0(r) \approx (1/2)[q(N+1)-q(N-1)]=(1/2)[q(\text{Anion})-q(\text{Cation})]$$

radical attack.

The condensed softness, s, which is often the DFT descriptor given for evaluating regioselectivity, is related to the Fukui functions by:[10]

$$s^- = S f^-$$
$$s^+ = S f^+$$

To evaluate regioselectivity, with similarities to matching FMO orbital coefficients, a local softness matching approach is effective at predicting the fa-

vored interaction orientation leading to the lower energy transition state. Essentially, predicting regioselectivity with softness matching corresponds to satisfying the HSAB theorem by matching the atomic sites with the closest softness values. Figure 3 shows the

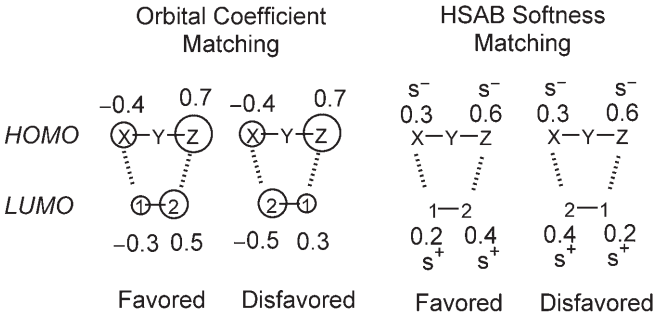

Figure 3. Hypothetical FMO orbital coefficient and HSAB softness matching schemes to evaluate regioselectivity.

corollary of softness matching with that of orbital coefficient matching for the hypothetical example of a nucleophilic 1,3-dipole interacting with an electrophilic alkene. As can be seen in Figure 3 the largest electrophilic attack softness value (meaning the most nucleophilic site), s^-, on the dipole is matched with the largest nucleophilic attack softness value (meaning the most electrophilic site), s^+, of the alkene in the favored interaction orientation. The alternative, disfavored orientation matches the largest values with the smallest values, and it is easy to see that this would not correspond to the softest interactions occurring to satisfy the HSAB principle. Whether to use the nucleophilic or electrophilic softness attack values for each of the reactants is based on the difference in chemical potential or evaluating electron transfer based on ionization potentials and electron affinities.

In the most representative example of applying softness matching and the HSAB principle, Chandra, Uchimaru, and Nguyen investigated the cycloadditions of hydrazoic acid and methyl azide with fluoro-, chloro-, methyl-, hydroxy-, and cyano-substituted ethylenes.[22] Using computed B3LYP ionization potentials and electron affinities of the neutral and charged dipoles and dipolarophiles, they showed that azides act primarily as electrophiles, except for the cycloadditions with cyanoethylene. Therefore, the local softness values for nucleophilic attack (s^+) for azide and methyl azide were matched with the local softness values for electrophilic attack (s^-) of the alkenes. For cyanoethylene, the opposite local softness attacks were considered. Scheme 1 gives the atomic softness values that were used to predict regioselectivity. As can be readily seen from the values in Scheme 1, for azide and methyl azide, the unsubstituted N terminal is the most electrophilic terminal with the largest nu-

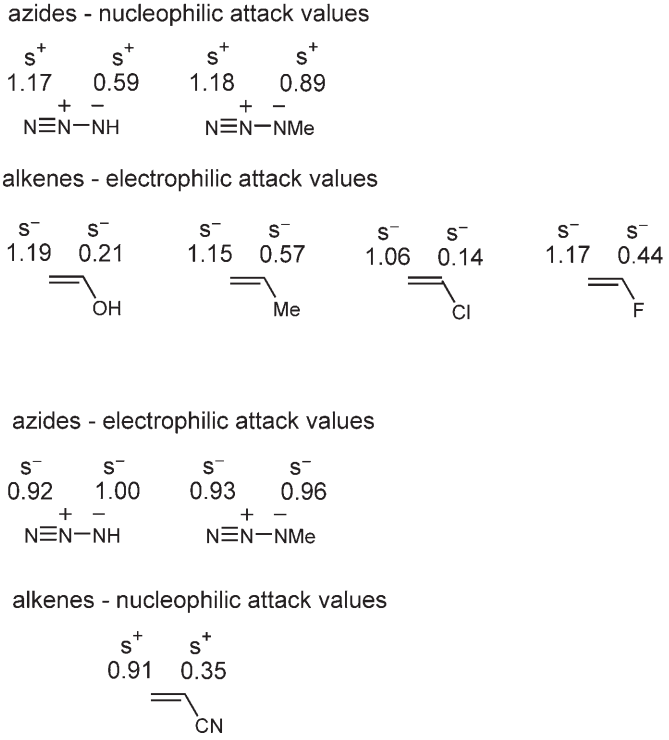

Scheme 1. Atomic softness values for azide, methylazide, and substituted alkenes. Values taken from ref.[22]

cleophilic attack value (s^+), while the substituted terminal is the least electrophilic terminal. For the alkenes considered, the unsubstituted carbon is the most nucleophilic with the largest electrophilic attack (s^-) value. This means that the unsubstituted carbon has a greater ability to stabilize developing positive charge, and therefore the preferred regioisomers are those that unite the unsubstituted azide terminals with the unsubstituted alkene carbons. This also satisfies the HSAB principle, creating the softest possible interactions. For cyanoalkene, using the opposite nucleophilic and electrophilic attack values, shows a reversal in regioselectivity, where the substituted terminal of azide and methyl azide unite with the unsubstituted cyanoalkene carbon. The most nucleophilic substituted end of the azides unites with the unsubstituted end of cyanoalkene, which carbon can accommodate the developing negative charge.

Softness matching is commonly done using the sum of the squared difference in atomic softness values for the regioisomers. For the reactions considered in Scheme 1, the squared difference in softness values correspond to the regioselective preference compared to the computed B3LYP barriers.[22]

Nguyen et al. have also investigated the regioselectivity of the diazonium betaines of with halogen-substituted acetylenes and cyanides in a similar fashion.[23] In another study, Chandra and Nguyen, have investigated the reactivity and regioselectivity of di-

azomethane, hydrazoic acid, methyl azide, and fulminic acid with HCP and $(H_3C)CP$ dipolarophiles.[24,25] They used the electrophilic attack values for the dipoles and nucleophilic attack values for the dipolarophiles. Scheme 2 shows a few examples of their regioselectivity analysis for diazomethane, hydrazoic acid, and fulminic acid with HCP. Softness matching shows that N-C (O-C) and C-P interactions are preferred over N-P (O-P) and C-C interactions. The methylene terminal of diazomethane is more nucleophilic and can stabilize developing positive charge, while the phosphorus atom of HCP is very soft, and can easily stabilize the developing negative charge. The values of the squared difference in softness show numerically the preference in regioselectivity for this reaction as well as the reactions with hydrazoic acid and fulminic acid. The squared difference values magnify the slight difference in electrophilic attack value of hydrazoic acid and fulminic acid. This qualitative result is in agreement with the computed difference in barrier heights. However, the squared difference values do not quantitatively relate to $\Delta\Delta E^{\ddagger}$.

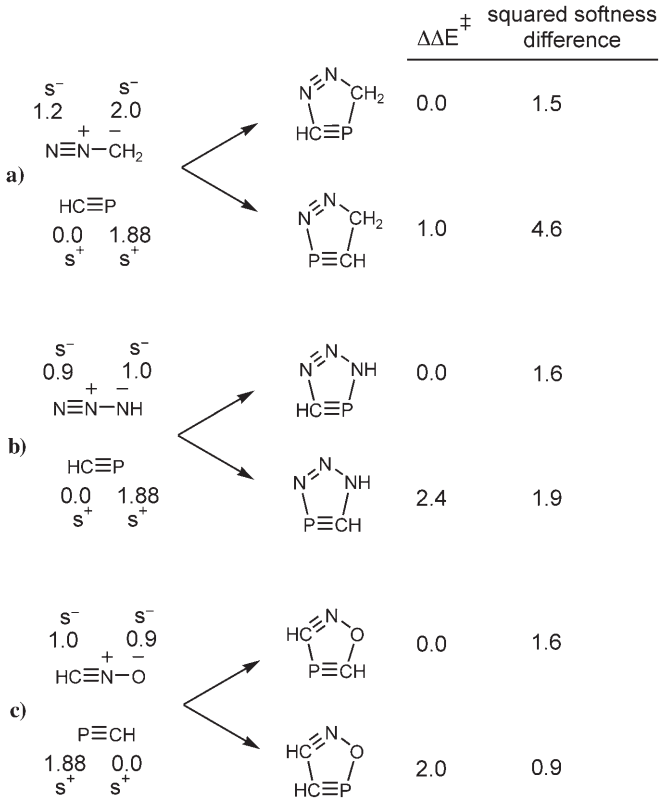

Scheme 2. Regioselective analysis for the cycloadditions of (**a**) diazomethane, (**b**) hydrazoic acid, and (**c**) fulminic acid with HCP. Electrophilic and nucleophilic softness attack values as well as the sum of the squared softness difference values and relative barrier heights in kcal mol^{-1} (B3LYP/6-31G**).[24]

These reactions provide important examples of application of the HSAB principle to understand regioselectivity; carbon and phosphorus atoms have similar FMO coefficients in both the HOMO and LUMO of HCP, and it is difficult to predict regioselectivity from an FMO approach.[24] Softness values are independent of frontier orbitals and correspond to the system as a whole, and have the potential to be more generally applicable than FMOs. The drawback is that no single generalization about which atoms are softer in cycloadditions has been developed.

An example using softness matching for Diels–Alder reactions was reported by Damoun et al. They investigated the [4+2] reactions of terminally monosubstituted 1,3-butadienes with monosubstituted ethylenes (Scheme 3).[26] Reactions of 1-substituted dienes with unsymmetrical dienophiles are of interest because replacement of an electron-withdrawing group with a donating group does not influence the regioselectivity.[27] Using the HF/3-21G method, they matched the local softness values for the *ortho* and *meta* regioisomers, and found that the vast majority of the 48 reactions had a smaller difference in softness for the *ortho* regioisomer than the *meta* one. This is in agreement with experimental results that give the *ortho* form as the major regioisomer.

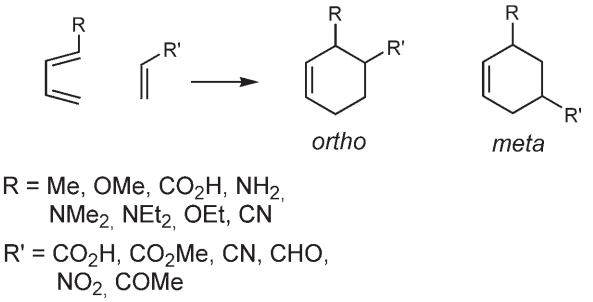

Scheme 3. The *ortho* and *meta* regioisomers of Diels–Alder cycloadditions of monosubstituted butadienes and ethylenes.

Herrera et al. have investigated, experimentally and theoretically, the highly regio- and stereoselective 1,3-dipolar cycloaddition reactions of captodative 1-acetylvinyl carboxylates **2.1** with arylnitrones **2.2** and other 1,3-dipoles (Scheme 4).[28] They showed that regioselectivity is controlled because the electron-donating groups in the captodative olefins increase the interaction between the nitrone carbon atom and the β-C1 carbon of the α,β-unsaturated ketone. This subtle stereoelectronic effect was reflected in the electrophilic attack values of the nitrone carbon atom and the C1 atom of the captodative olefins. For the non-captodative methacrolein dipolarophile, this interaction is significantly lower because there is no longer a large nucleophilic tendency at C1. Therefore all regioselectivity is lost.[29]

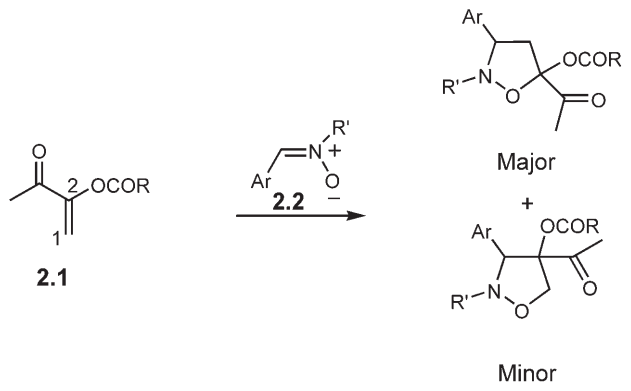

Scheme 4. Captodative 1,3-dipolar cycloadditions of 1-acetylvinyl carboxylates.

Chemical potential, hardness, and softness, can be used to calculate the interaction energy, ΔE_{int}, to compare the reactivities of dipolarophiles with 1,3-dipoles. These equations were first generalized by Parr and Gázquez and then extended for atomic interactions by Méndez and Gázquez.[19,20] The equation below is the approximate interaction energy between molecules A and B, where μ and S are the respective chemical potentials and softness values, and λ is a constant related to the number of valence electrons that are involved in the interaction.

$$\Delta E_{int} = (-1/2)\frac{(\mu_A - \mu_B)^2}{S_A + S_B} S_B S_A - (1/2)\frac{\lambda}{S_A - S_B}$$

Méndez, Tamariz, and Geerlings have used this equation for the reaction of benzonitrile oxide with vinyl *p*-nitrobenzoate and its acetyl derivative **2.7** that form isoxazolines **2.5** and **2.6** and **2.8** and **2.9**, respectively (Scheme 5).[30] Experimentally, the reaction of **2.3** with **2.7** gives exclusively the 5-acetyl-3-arylisoxazole **2.8**. Using the molecular values of μ and S to calculate ΔE_{int}, benzonitrile oxide has a 2.2 kcal mol^{-1} larger interaction energy with **2.7** than **2.4**. Using the local version of the ΔE_{int}, for the possible regioisomeric interactions, the maximum interaction occurs when the C1 atom from **2.4/2.7** acts as the nucleophile towards the electrophilic carbon atom of benzonitrile oxide.

Ponti and Molateni have investigated 1,3-dipolar cycloadditions using a generalization of the HSAB principle in a semiquantitative manner by computing the grand potential, Ω, defined as, E−Nμ. E is the energy, N is the number of electrons, and μ is the chemical potential.[31] This grand potential is a measure of stabilizing interactions between two molecules. They used this approach to investigate cycloadditions

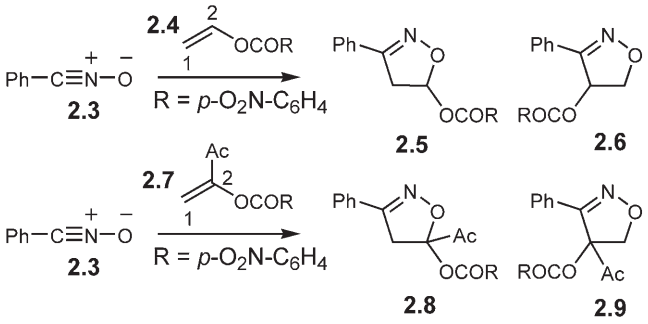

Scheme 5. Cycloaddition of benzonitrile oxide with vinyl *p*-nitrobenzoate and its acetyl derivative.

of *C*-carbomethoxy-*N*-(4-substituted)phenylnitrilimines **2.10**, aryl azides **2.11**, and (4-substituted)benzonitrile oxides **2.12** with methyl propiolate **2.13** shown in Scheme 6.[32–35]

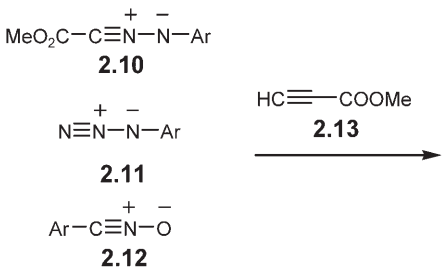

Scheme 6. 1,3-Dipolar cycloadditions with methyl propiolate.

The ΔΩ values correctly predict the preferred regiochemistry preference for all reactions considered. The authors also showed that ΔΔΩ is proportional to the barrier heights and this correlation can be used to estimate product ratios between the regioisomers. The strong correlation to the barrier height was attributed to the fact that ΔΩ accounts for most of the energy difference between the regioisomeric transition states.

The following examples show the usefulness of another conceptual DFT descriptor called the electrophilicity index. First suggested by Maynard,[36] and then refined by Parr,[37] the so-called "electrophilicity index" ω, has been used as a measure for reactivity for a variety of reactions including 1,3-dipolar and Diels–Alder cycloadditions.[38] ω is the chemical potential squared divided by two times the hardness value.

$$\omega = \mu^2/2\eta$$

Similar to the electron affinity, ω is a measure of the capability of a molecule to accept electrons. A large chemical potential, μ, reflects the tendency to acquire charge, and a small η value indicates a good electrophile.

In a series of papers, Domingo, Pérez and co-workers have investigated a variety of cycloaddition reactions using the global electrophilicity index. They characterized the most important 1,3-dipoles as strong, moderate, or marginal electrophiles according to their ω values.[39] Domingo and Contreras have also characterized a series of dienes and dienophiles commonly used in Diels–Alder cycloadditions.[40]

This index and classification have been promoted as a method to decipher the charge transfer direction between addends and predict concerted or asynchronous pathways based on the difference between ω values of a dipole/dipolarophile pair. The difference in the electrophilicity index Δω between dienes and dipolarophiles has been postulated to be an indicator of the polarity of a cycloaddition mechanism.

A representative application of the electrophilicity index was reported by Domingo and co-workers who investigated the polarity of Diels–Alder cycloadditions between cyclopentadiene and mono-, di-, tri-, and tetracyanoethylenes.[41] Scheme 7 shows the ω values for cyclopentadiene and cyanoethylenes. Cyclopentadiene has a lower value of ω and shows that the direction of charge transfer is from diene to cyanoethylenes. The increasing ω values are in accord with the charge transfer to the alkene at the transition states. The electrophilicity values indicate the increasing polar character for these reactions and the large rate enhancements found experimentally.

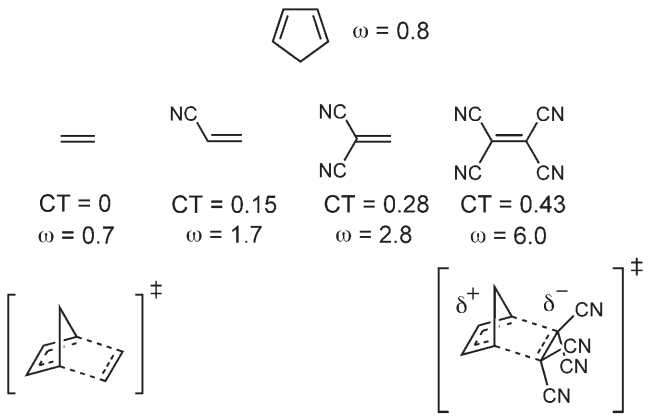

Scheme 7. Charge transfer to ethylenes and electrophilicity index values for ethylenes for reactions of cyclopentadiene with ethylene, mono-, di-, and tetracyanoethylenes.[41]

A similar approach using an electrophilicity index was also applied to the polar Diels–Alder reactions of nitrosoalkenes with enamines,[42] and 1,3-butadienes with dimethyl acetylenedicarboxylate.[43] Domingo also showed that the low Δω values for the reactions of benzonitrile oxide with alkynylboronates explains the non-polar character of these transition states.[44]

A global electrophilicity analysis was also carried out on a number of Lewis acid-catalyzed reactions showing that ω is a good predictor of Lewis acid polarization. Aluminum halide Lewis acid catalysts for reactions of nitroalkenes with vinyl ethers,[45] and boron heterocycle Lewis acid catalysts for the Diels–Alder reactions of cyclopentadiene and methylacrolein have also been investigated.[46] Domingo also applied this method to the Lewis acid-catalyzed reactions of *N*-acetyl-1-aza-1,3-buadiene with dimethylvinylamine,[47] and cyclopentadiene with arylidenoxazolone.[48] Ruano et al. showed that the increased reactivity of 5-ethoxy-3-*p*-tolylsulfinylfuran-2(5*H*)-one *versus* 5-methoxyfuran-2(5*H*)-one towards diazoalkanes could be rationalized based upon an electrophilicity index difference.[49]

In a different approach, Noorizadeh and Maihami have investigated the regioselectivity of 67 cycloaddition reactions using the electrophilicity index of the reaction products rather than the reactants. They found that the major product always had a lesser electrophilicity value; however, these results seem to be basis set dependent.[50]

The electrophilicity index, ω, also has a local equivalent, ω_k, which can be used to analyze regioselectivity.

$$\omega_k = \omega f_k^+$$

A number of studies have applied the combination of electrophilicity index model with local softness or Fukui function values to rationalize reactivity and regiochemistry.[51] Scheme 8 shows the values reported

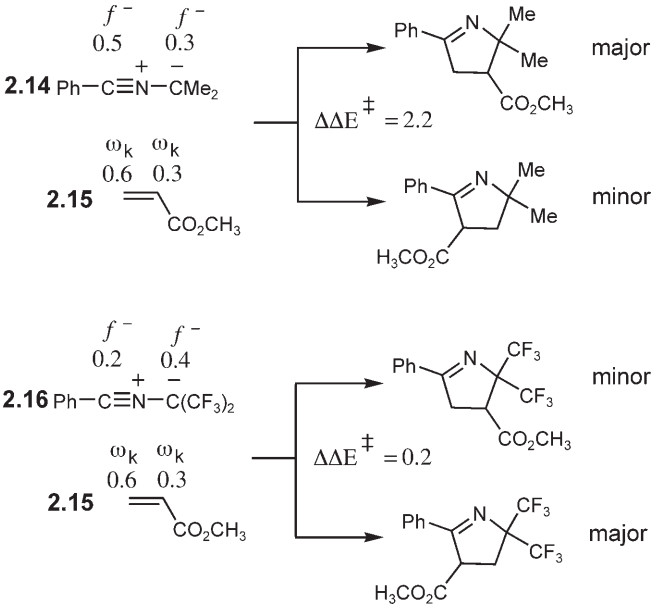

Scheme 8. 1,3-Dipolar cycloadditions of nitrile ylides to methyl acrylate. Electrophilic attack Fukui functions on the 1,3-dipole terminals and atomic electrophilicity index, ω_k for the dipolarophiles are given, along with the B3LYP/6-31G* $\Delta\Delta E^{\ddagger}$ values the regioisomers.[52]

by Aurell et al. for nitrile ylide **2.14** and **2.16** addition to methyl acrylate.[52] Methyl acrylate is considered a strong electrophile, and has a larger local electrophilicity value at the β-position, and is the preferred site of nucleophilic attack. For dimethylphenylnitrilium ylide **2.14**, the Fukui function for electrophilic attack shows that the dipole terminal that is phenyl-substituted is more nucleophilic. Matching these values leads to a correct prediction of the major regioisomer in accord with the computed difference in barriers. This example also highlights the sensitivity of the Fukui function to predict the reversal of polarization and regioselectivity for CF_3-substituted nitrile ylide **2.16** shown in Scheme 8. The CF_3 groups localize the negative charge and increase the nucleophilicity at that dipole terminal. This approach can only account for regioselective preference and does not necessarily correspond quantitatively to the difference in barrier heights.

Merino, Rescifina and co-workers have also rationalized the regiochemistry of *C*-(methoxycarbonyl)-*N*-methylnitrones with methyl acrylate and vinyl acetate,[53] and the nitrile oxide addition to anthracene and acridine using a similar approach.[54] Local electrophilicity has also been a successful criterion for rationalizing the regioselectivity for the Diels–Alder reaction of cyclopentadiene and 4-aza-6-nitrobenzofuroxan.[55]

In conclusion of this section, we note that Gayatri and Sastry have assessed the performance of DFT descriptors for 64 Diels–Alder reactions shown in Scheme 9 for predicting regioselectivity.[56] Using Fukui function matching from B3LYP calculations, 53 of 64 reactions could be rationalized by this approach. This highlights the potential broad applicability of DFT descriptors to predict reactivity and selectivity, but also the approximate nature of these descriptors.

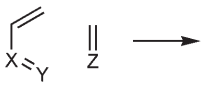

X = N, P, CH
Y= NH, PH, O, S, CH_2
Z = NH, PH, O, S, CHMe, CHOH, CHCN, CHCHO

Scheme 9. Regioselective Diels–Alder cycloadditions assessed using FMO coefficients and DFT descriptors.

2.3 Configuration Mixing Models

The qualitative valence-bond configuration mixing model of Pross and Shaik describes reaction pathways based on mixing of ground and excited state configurations rather than orbital or density interactions.[57] The transition state, and reaction pathway, are functions of the configurations considered and the extent to which they mix. This model, as implemented for cycloaddition reactions, focuses on the specific bonds that are broken and formed and their spin configurations. The barrier results from the crossing (or avoided crossing of states) of the reactants and product spin configuration wavefunctions. Figure 4 shows this

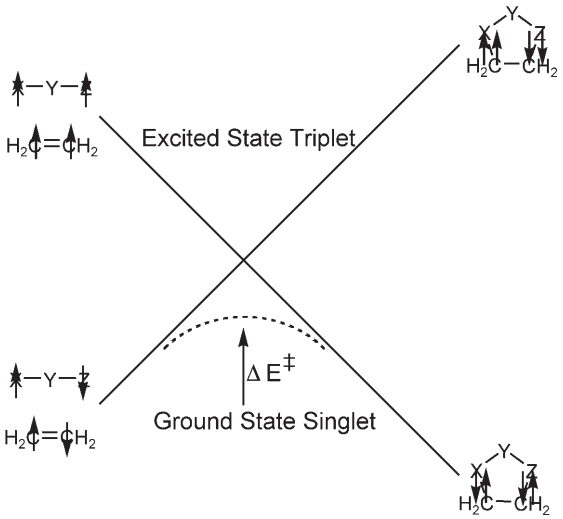

Figure 4. Configuration mixing model for 1,3-dipolar cycloadditions.

crossing and the resulting barrier for 1,3-dipolar cycloadditions with ethylene. Essentially, the singlet ground state of the 1,3-dipole and ethylene lead to the triplet excited state of the product, while the excited state triplet of the reactants leads to the singlet product ground state. Therefore, during the reaction, the intramolecular spin paired electrons in the 1,3-dipole and ethylene must decouple (transition from singlet to triplet spin states) to allow for the formation of the intermolecular spin paired σ-bond. Because the barrier height is controlled by the avoided curve crossing of the singlet and triplet states of the bonds that are formed and broken, it has been postulated that reactivity should correlate with the singlet-triplet energy gap (ΔE_{ST}) of the reactants. Therefore, the lower the ΔE_{ST}, the lower the barrier, the earlier the TS, and the greater is the exothermicity of the reaction energy. This is an elegant way of showing why increasing diradical character (which is related to decreasing the singlet-triplet gap) leads to high reactivity.

Su et al. investigated the reactions of nitrous oxide, hydrazoic acid, diazomethane, fulminic acid, formonitrile imine, and formonitrile ylide, the six prominent 1,3-dipoles "with a double bond", with ethylene using B3LYP and CCSD(T) methods.[58] They used CCSD(T) ground state singlet-triplet energy gaps (ΔE_{ST}) for these six 1,3-dipoles to rationalize barrier trends and reaction energies in a qualitative manner,

since the ΔE_{ST} value for ethylene is constant. The ΔE_{ST} ($\Delta E^{\ddagger}$ in parenthesis) values are 55.6 (28.7), 45.3 (13.2), 32.0 (12.8), 64.4 (11.2), 38.1 (6.3), and 27.2 (5.1) kcal mol^{-1}, respectively. A higher barrier and less exothermic reaction is associated with a larger ΔE_{ST} value for the diazonium and nitrilium betaine series, but there is not a linear correlation or general relationship.

In a related study, Liao et al. investigated the cycloaddition of nitrile ylide with cyano-, nitro-, chloro-, hydroxy-, and methyl-disubstituted ethylene derivatives.[59] They found that the lowest barriers were associated with highly electron-withdrawing groups. Using B3LYP, they observed that the smaller the ΔE_{ST} value, the lower the barrier. This general trend in reactivity is also observed in the ethylene HOMO–LUMO gaps. The lower barriers for electron-withdrawing groups were rationalized by the stabilization of the π^* orbital, which decreases the singlet-triplet splitting. This trend has also been rationalized by the favorable HOMO–LUMO interaction when the electron-rich nitrile ylide interacts with electron deficient dipolarophile.

Sakai and Nguyen have employed the so called "CAS-LMO-CI" method (complete active space-localized molecular orbital-configuration interaction) to investigate the contributing electronic configurations for the dipolar cycloadditions of diazomethane and fulminic acid with acetylene.[60,61] This method utilizes a full configuration interaction calculation on a localized (atomic) CASSCF/6-31G* wavefunction. The relative weights of localized molecular orbitals are analyzed along the minimum energy pathway (MEP). This type of treatment gives insight into the electronic reorganization along the reaction pathway, and the multi-reference wavefunction should give an accurate description of contributing configurations. Scheme 10 shows three possible electronic mechanisms possible for dipolar cycloadditions as defined by Sakai. **I** depicts a spin-coupled bond breaking and bond formation, a type of biradical coupling mechanism. **II** and **III** are "heterolytic" mechanisms, where the pairs of electrons migrate to form the new bonds, with **II** and **III** differing in direction of electron flow. This method provides a quantum mechanical version of the organic chemists' famous "arrow-pushing" formalism.

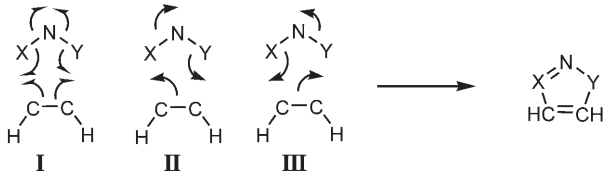

Scheme 10. Three electronic mechanisms for 1,3-dipolar cycloadditions.

When the CAS-LMO-CI method was applied to fulminic acid and diazomethane plus acetylene, two electron configurations had the largest change along the MEP (Figure 5). Configuration **A** decreased dramatically on going from reactants to products, while configuration **B** increased in weight along the minimum energy path. Based on this analysis, the authors concluded that the reaction mechanisms proceed through the coupling of biradical structures with slight charge polarization. For fulminic acid, the electron is initially transferred from the oxygen to the central nitrogen, and for diazomethane, electron movement occurs from the carbon atom to the central nitrogen.

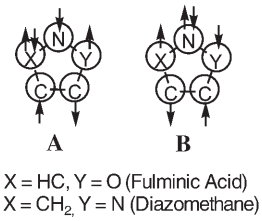

Figure 5. Configurations **A** and **B** describe the two major configurations at the transition state for fulminic acid and acetylene.

The reactions of fulminic acid and diazomethane with NCH, HCP were also investigated. Depending on the nature of the dipolarophile, a diradical coupling or ionic type mechanism occurs. Ionic, heterolytic mechanisms were found for the reactions of HCNO and diazomethane with HCN were the new bonds had a large electronegative difference.[61]

Sakai has also used the CAS-LMO-CI method to investigate the stepwise and concerted pathways for the cycloaddition of 1,3-butadiene with ethylene.[62] The concerted reaction pathway is dominated by a single configuration **CF1** (Figure 6). In general, the largest weighted configurations for the reactants (**CF2–4**) correspond to π bonds in the Kekulé structure of butadiene and ethylene. These configurations decrease along the reaction pathway, while configurations **CF6–8** increase and correspond to the new σ bonds and π bond. Sakai points out that, at the transition state, configurations **CF2–7** are equally weighted, and this corresponds to its aromatic and concerted nature.

Karadakov et al. have used the spin-coupled CASSCF(6,6)/6-31G* method to investigate the electronic mechanisms for Diels–Alder and 1,3-dipolar cycloadditions.[63,64] For the cycloaddition of 1,3-butadiene with ethylene they found that a biradical coupling mechanism operates where three π bonds break and recouple to form two σ bonds and a π bond.[65] When this same method was employed to investigate

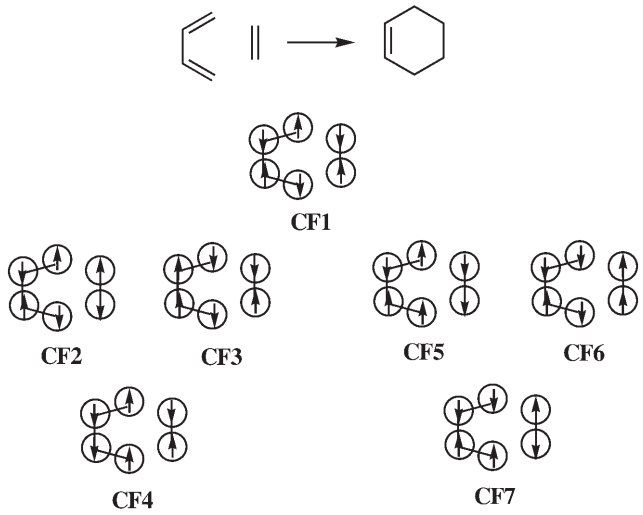

Figure 6. Most important configurations for 1,3-butadiene with ethylene and cyclohexene for the Diels–Alder cycloaddition.

the reaction of fulminic acid addition to acetylene, they found that three orbitals shift to create the two new bonds and the lone pair, which corresponds to the heterolytic mechanism **II** from Scheme 10. This is opposite to the predicted configurations by Sakai and co-workers. These studies have stimulated a mechanistic debate and culminated in two commentaries, and another investigation by Harcourt and Schulz. These authors advocate, opposed to the results of Karadakov et al., that fulminic acid and nitrous oxide have pentavalent nitrogens, and a valence bond consideration gives evidence for biradical coupling.[66,67]

Whatever the outcome of these investigations, there seems little doubt that the 1,3-dipolar and Diels–Alder cycloadditions have aromatic transition states that at least formally correspond to the union of two diradical wavefunctions.

Models to quantitatively define bonding in terms of σ-bonds, π-bonds, and lone pairs, typically conveyed in Lewis structures have also been developed and applied to cycloadditions. Polo et al. has used the electron localization function (ELF) method to investigate the mechanism of fulminic acid with acetylene,[68] while Berski et al. used ELF to investigate the reaction of 1,3-butadiene with ethylene.[69]

Weinhold's natural resonance theory (NRT) has also been applied by Mawhinney et al. towards understanding the electronic structure of nitrilimines.[70] They concluded that nitrilimines had significant carbene character. However, Ponti and co-workers have used CASSCF and spin-coupled calculations to show that the most important electronic structure of nitrilimines corresponds to the propargylic resonance form with little or no carbenic character.[71]

3 Quantitative Computation of Activation Barriers and Reaction Energetics

Only recently have experimentally accurate (defined as absolute error of $\pm 1\,\mathrm{kcal\,mol^{-1}}$)[72] quantitative treatments of cycloadditions become possible by using compound quantum mechanical methods such as the G_n, CBS_x, or W_n series of methods.[73] These compound methods use successive quantum mechanical methods and empirical corrections to give the accurate thermochemistry values, albeit at a high computational cost. It is not feasible to use these methods on large systems of experimental interest. Density functional theory has become the attractive alternative because of its remarkable balance of speed and accuracy.[74] DFT has become the primary theoretical method for theoretical investigations of cycloadditions.[75] However, does DFT, especially the popular B3LYP, give experimentally accurate kinetic and thermodynamic energies? Recently, many investigations have been devoted to testing the performance of DFT methods for bond dissociation energies,[76] enthalpies of formation,[77] enthalpies of atomization,[78] proton affinities,[79] hydrogen abstraction reactions,[80] radical reactions,[81] weak interactions,[82] S_N2 reactions,[83] pericyclic reactions,[84,85] organic reactions,[86,87] metals,[88] materials,[89] biological applications, and even reactions relevant to astrophysics.[90]

This section reviews investigations that give the most reliable quantitative thermochemistries for Diels–Alder and 1,3-dipolar cycloadditions. Benchmark investigations of cycloadditions that give critical evaluations of the accuracy and precision of *ab initio* and DFT methods are also reviewed.

The quantitative prediction of activation barriers and reaction energies for Diels–Alder reactions in our laboratory has culminated with the proposal of a test set of hydrocarbon pericyclic reactions, including electrocyclic reactions, sigmatropic shifts, cycloadditions, and cycloreversions (Scheme 11), to be used as a standard to benchmark the performance of methods. Our lab has compared compound, *ab initio*, and DFT quantum mechanical methods to experimental activation barriers and reaction energies for this hydrocarbon test set.[91]

In this test set, reactions **3.7–3.9** are the cycloadditions of 1,3-butadiene with ethylene **3.7**, cyclopentadiene with ethylene **3.8**, and cyclopentadiene dimerization **3.9**. The experimental activation and reaction energies for **3.7–3.9**, corrected to 0 K using B3LYP thermochemical values, along with the values from the most accurate methods are listed in Table 1. Also listed is the mean absolute deviation (MAD) of activation (reaction) enthalpies for these methods for the entire hydrocarbon pericyclic test set, which give a good estimate of the accuracy.

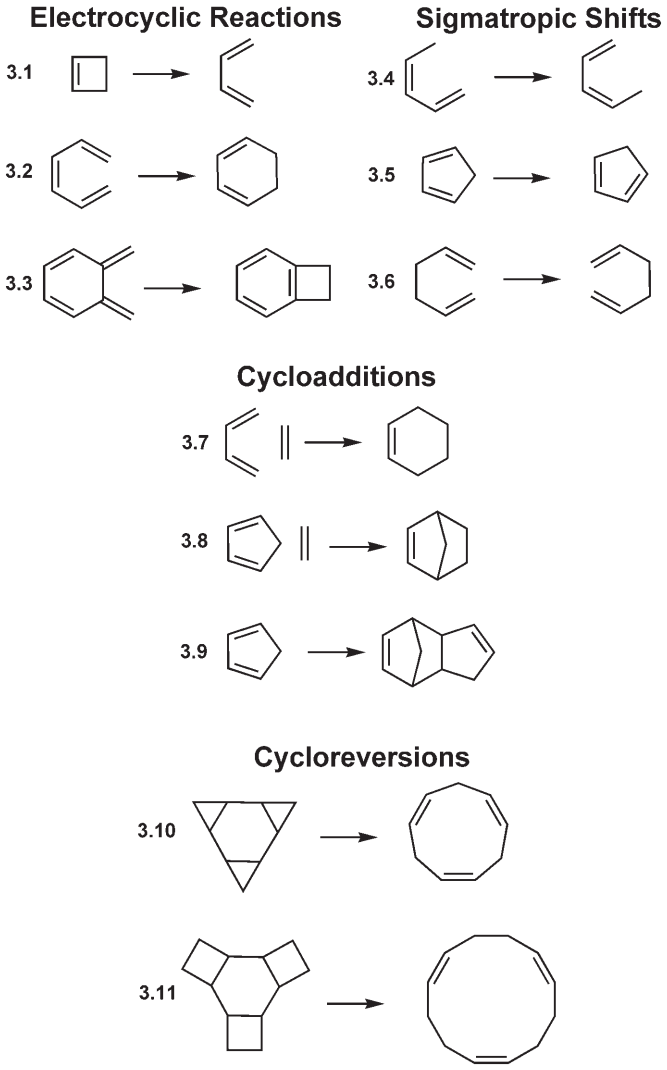

Scheme 11. The standard set of hydrocarbon pericyclic reactions **3.1–3.11** used for benchmarking purposes.

The methods in Table 1 are listed in order of increasing MAD value for $\Delta H^{\ddagger}$ compared to experiment. The hybrid DFT methods, B3LYP, MPW1K, and O3LYP along with the compound CBS-QB3, and CASPT2 all give MAD values under 2.5 kcal mol^{-1} and essentially statistically perform equivalently.[90,92] Linear correlations between experimental and computed $\Delta H^{\ddagger}_{rxn(0K)}$ values indicates that CBS-QB3 and CASPT2 methods gives the best agreement with experiment. B3LYP gives good agreement with experiment, but does not agree well with CBS-QB3 and CASPT2 for **3.8** and **3.9**. For reaction energies, CBS-QB3 and CASPT2 show superior performance with MAD values of 1.6 kcal mol^{-1}, while DFT methods range from 3.9 to 6.2 kcal mol^{-1}. See ref.[93] for a brief description of these methods.

For the cycloaddition of 1,3-butadiene with ethylene, CASPT2 gives the exact $\Delta H^{\ddagger}$ value, and B3LYP only underestimates the barrier by 0.1 kcal mol^{-1}. In general, DFT methods have a small deviation from experiment (-0.6 to $+1.8$ kcal mol^{-1}) for $\Delta H^{\ddagger}$. For the reaction energy, only MPW1K deviates substantially. CBS-QB3 and CASPT2 underestimate the barriers (-6.4 and -5.1 kcal mol^{-1}) for reaction **3.8**, while DFT methods deviate only slightly (-3.1 to $+0.2$). Only CBS-QB3 gives an accurate reaction energy with a deviation of -1.4 kcal mol^{-1}. The computed activation barriers for cyclopentadiene dimerization have a large range (12.7 to 24.1 kcal mol^{-1}), while experimental measurements have a range of 4.6 kcal mol^{-1}. The highly overestimated B3LYP value may be due to the systematic error for calculating norbornene structures and may be due to the inability of B3LYP to correctly predict the strain in norbornene structures or simply account for the proper electron correlation.[94] The CBS-QB3 and CASPT2 values of 11.6 and 12.7 kcal mol^{-1} may be a more accurate estimate of the barrier, and are close to gas phase measurements.

Morokuma and co-workers have also used high accuracy methods, CCSD(T), G2MS and G2MP2 to quantitatively investigate the barriers of butadiene with ethylene and acetylene **3.7a** and **b** and cyclopentadiene with ethylene and acetylene **3.8a** and **b**.[95]

Table 1. Experimental and computed $\Delta H^{\ddagger}_{rxn(0K)}$ and $\Delta H_{rxn(0K)}$ values for *ab initio*, DFT, and CBS-QB3 methods, along with the mean absolute deviation (MAD).

Reaction	**3.7**		**3.8**		**3.9**		MAD
	$\Delta H^{\ddagger}$	ΔH_{rxn}	$\Delta H^{\ddagger}$	ΔH_{rxn}	$\Delta H^{\ddagger}$	ΔH_{rxn}	$\Delta H^{\ddagger}$ (ΔH_{rxn})
Experimental[a]	25.0	−39.6	23.7	−23.2	15.9	−19.7	
B3LYP/6-31G*	24.9	−36.6	22.2	−18.6	21.1	−11.1	1.5 (4.1)
MPW1K/6-31+G**	24.4	−28.4	20.6	−30.3	19.2	−23.7	2.1 (6.2)
CBS-QB3	22.9	−38.3	17.3	−24.6	11.6	−22.2	2.3 (1.6)
O3LYP/6-31G*	26.8	−37.3	23.9	−19.7	24.1	−11.4	2.4 (3.9)
CASPT2/6-31G*//CASSCF	25.0	−39.7	18.6	−26.2	12.7	−24.2	2.4 (1.6)

[a] The experimental error ranges for reaction **3.7** is ± 0.5 and ± 1 kcal mol^{-1} for the activation and reaction energies respectively. For **3.8**, the error range is ± 1.6 kcal mol^{-1} for the activation energy. For cyclopentadiene dimerization, **3.9**, see ref.[91] for a liberal discussion of the experimental error.

These values and the previously mentioned CBS-QB3 values are compared in Scheme 12. For the reaction of butadiene with ethylene, the G2 variants and CBS-

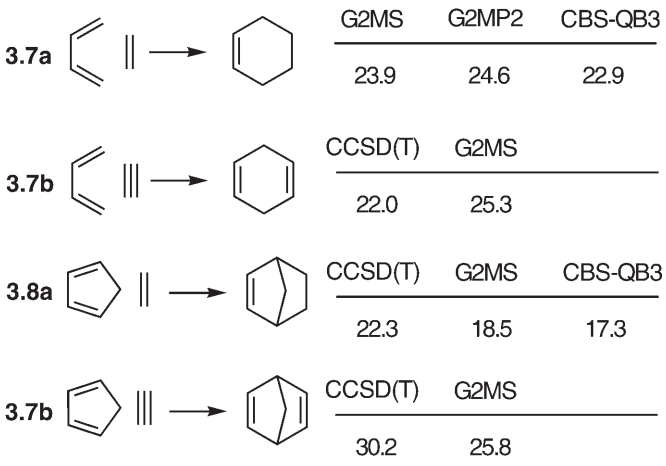

Scheme 12. Summary of highly accurate methods for the barriers of butadiene and cyclopentadiene with ethylene and acetylene.[90,91,94]

QB3 agree very well on a converged value of about 24 kcal mol^{-1}. For the other reactions shown in Scheme 12, the CCSD(T) values deviate from the G2MS and CBS-QB3 values. The G2MS and CBS-QB3 for cyclopentadiene and ethylene show a converged value of about 18 kcal mol^{-1}.

Sastry and co-workers investigated the reactions of 1,3-butadiene, cyclopentadiene, furan, thiophene, pyrrole, silole, and phosphole with ethylene using semi-empirical, *ab initio* and DFT methods (Scheme 13).[96]

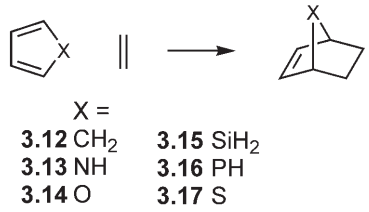

Scheme 13. Cyclic diene [4+2] reactions that were benchmarked by comparison to experimental and G3 values.

They found that all methods were qualitatively able to reproduce barrier trends for these reactions, but Hartree–Fock and MP2 methods were quantitatively unreliable, while B3LYP and MP3 compared well to experiment and the CCSD(T) method.

Goumans et al. quantitatively accessed these same reactions with very accurate methods including the compound G3 method and QCISD(T).[97] The B3LYP, MP2, and spin-component-scaled MP2 (SCS-MP2)[98] methods were compared to these highly accurate methods. The most accurate methods, G3, CCSD(T), and QCISD(T) values are listed in Table 2 along with the mean average error (MAE) and maximum error for the B3LYP, MP2, and SCS-MP2 methods compared to the G3 values for activation and reaction energies combined. B3LYP and MP2 both perform somewhat poorly, while the SCS-MP2 method performs very well with a very large 6-311++G(3df,3pd) basis set.

A recent investigation by Jones et al. compared activation barriers computed by B3LYP, MPW1K and Hartree–Fock methods for the Diels–Alder reactions of cyclopentadiene and 9,10-dimethylanthracene with

Table 2. G3, CCSD(T), and QCISD(T) activation and reaction energies for cyclic dienes with ethylene, along with the mean average error (MAE) and maximum error for the B3LYP, MP2, and SCS-MP2 methods compared to the G3 values.

		3.7	**3.12**	**3.13**[e]	**3.14**	**3.15**	**3.16**[f]	**3.17**
G3[a]	ΔE^{+}	24.4	18.8	28.8	23.7	17.1	21.4	31.3
	ΔE_{rxn}	−37.8	−24.2	0.1	−10.2	−25.2	−19.9	−6.3
CCSD(T)[b]	ΔE^{+}	25.1	19.8	28.3	24.7	19.8	23.6	32.7
	ΔE_{rxn}	−46.7	−31.0	−7.7	−16.1	−30.2	−26.4	−13.7
QCISD(T)[a]	ΔE^{+}	27.4	21.9	30.6	26.7	21.5	25.3	34.5
	ΔE_{rxn}	−40.5	−25.2	−2.4	−11.1	−24.9	−21.0	−8.7
			MAE	Max. Error				
	B3LYP[c]		4.5	6.5				
	MP2[c]		5.4	9.2				
	SCS-MP2[d]		2.9	5.3				
			(1.1)	(2.4)				

[a] Values taken from ref.[96]
[b] Values taken from ref.[95], values do not include ZPE using the 6-31G* basis set. QCISD(T)/6-31G* at MP2 geometries, and include ZPE.
[c] 6-31G* basis set.
[d] 6-31G* and values in parenthesis are 6-311++G(3df,3pd).
[e] *anti*-transition state.
[f] *syn*-transition state.

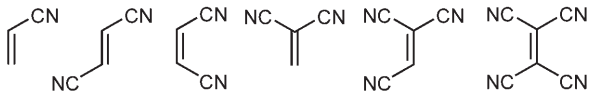

Scheme 14. Mono-, di-, tri-, and tetra-substituted ethylenes investigated for the Diels–Alder reactions with cyclopentadiene and 9,10-dimethylanthracene.

cyanoethylenes.[99] The cyanoethylenes considered in their investigation are shown in Scheme 14.

Hartree–Fock and MPW1K methods correctly predict the experimental activation enthalpy trends for the whole series, but B3LYP failed to predict the correct trends for **3.22** and **3.23**, with an increase in activation barrier for **3.22** and **3.23** compared to **3.21**, contrary to experiment (Table 3). These reactions have significant charge separation in the transition state, especially tetracyanoethylene, and methods with a larger fraction of exact exchange energy in the functional, such as MPW1K, perform best. For reaction enthalpies, HF and MPW1K perform well, while B3LYP underestimates the exothermicity.

Jones et al. also compared the activation barriers for 9,10-dimethylanthracene with 1,1,2,2-$C_2(CN)_4$. MPW1K performs well with an activation enthalpy of $-1.2\,kcal\,mol^{-1}$ compared to $1.2\,kcal\,mol^{-1}$ measured experimentally. B3LYP performs very poorly, deviating by $11.5\,kcal\,mol^{-1}$ from experiment. These results are similar to those reported by Hehre and Domingo et al.[100]

For 1,3-dipolar cycloadditions, Ess and Houk quantitatively investigated the reactions of ethylene and acetylene with the nine 1,3-dipoles shown in Scheme 15 using the highly accurate CBS-QB3 method for the activation and reaction enthalpies.[101] Because there are no reported experimental measurements for dipolar cycloadditions of ethylene and acetylene with **3.24–3.32**, and very few experimental systems that can be treated with high accuracy methods, the CBS-QB3 values are taken to be the most accurate and the values were used as a standard to benchmark other methods.

The CBS-QB3 $\Delta H^{\neq}_{(0K)}$ and $\Delta H_{rxn(0K)}$ values are listed in Table 4 along with the average errors for B3LYP, MPW1K and MP2 methods compared to these CBS-QB3 values. The performance of the

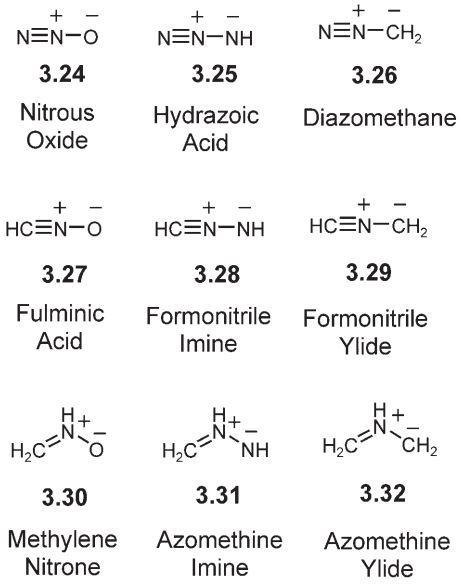

Scheme 15. Nine 1,3-dipoles from the three major classes.

B3LYP and MPW1K DFT methods was superb compared to CBS-QB3 for the computing of activation enthalpies as can be seen by MAD values of 1.5 and $1.1\,kcal\,mol^{-1}$. The reaction energetics were another story: B3LYP has a larger MAD, $2.4\,kcal\,mol^{-1}$, whereas MPW1K performed poorly with a MAD value of about $18\,kcal\,mol^{-1}$. The MP2 method gave the expected underestimation of barrier heights. All DFT methods performed more poorly with larger basis set.

Grimme et al. used these same CBS-QB3 values to evaluate the recently developed B2-PLYP DFT method and SCS-MP2 method.[102] Using the cc-pVTZ basis set, they found that SCS-MP2 performed very well for the activation energies of the 1,3-dipolar cycloadditions with a MAD value of $1.3\,kcal\,mol^{-1}$. This was a drastic improvement over the standard MP2 method with a $4.5\,kcal\,mol^{-1}$ MAD value with the same basis set. B2-PLYP performed better than B3LYP with 1.5 and $3.9\,kcal\,mol^{-1}$ MAD values respectively.

The reactions of diazonium and nitrilium betaines (**3.24–3.29**) with ethylene have also been treated with the CCSD(T) method by Su et al. (values given in Section 2.3). These values are close to the CBS-QB3 values. Two other studies have also applied the

Table 3. Activation barriers for the *endo*-Diels–Alder reactions of cyclopentadiene with cyanoethylenes.

Dieneophile		C_2H_4	3.18	3.19	3.20	3.21	3.22	3.23
Experimental	$\Delta H^{\neq}$	22.5	15.5	12.8	12.8	9.0	7.6	5.0
B3LYP	$\Delta H^{\neq}$	22.3	18.9	16.5	17.0	11.2	11.9	12.1
MPW1K	$\Delta H^{\neq}$	20.7	16.3	12.9	13.4	8.9	7.7	5.6
HF	$\Delta H^{\neq}$	42.0	37.8	34.4	34.5	30.0	28.0	26.1

Table 4. CBS-QB3 $\Delta H^{+}_{(0K)}$ and $\Delta H_{rxn(0K)}$ values for 1,3-dipolar cycloadditions of dipoles **3.24–3.32** with ethylene and acetylene, and the statistical comparison of DFT and *ab initio* methods against these values.

			3.24	3.25	3.26	3.27	3.28	3.29	3.30	3.31	3.32
CBS-QB3	ΔH^{+}	ethylene	27.9	20.3	14.6	13.0	7.2	5.9	13.8	7.8	0.9
		acetylene	27.9	20.1	15.2	14.1	8.5	7.4	14.0	7.6	1.5
	ΔH_{rxn}	ethylene	−4.4	−19.7	−31.7	−39.3	−57.4	−68	−28.8	−44.2	−62.7
		acetylene	−37.1	−61.5	−49.0	−74.0	−100.3	−86.7	−43.9	−59.5	−76.9
		MAD	MD	Error Range							
B3LYP[a]	ΔH^{+}	1.5	0.3	6.6							
	ΔH_{rxn}	2.4	−1.4	9.6							
MPW1K[a]	ΔH^{+}	1.1	0.3	4.1							
	ΔH_{rxn}	17.9	−17.9	42.2							
MP2[a]	ΔH^{+}	3.4	−3.0	8.5							

[a] 6-31G* basis set.

CCSD(T) method to the dipolar cycloaddition of diazomethane with ethylene. Blavins et al. computed a $\Delta H^{+}_{(0K)}$ value of 16.4 kcal mol^{-1} with the CCSD(T)/6-311++G(2d,2p) method,[103] while Branchadell found the barrier to be 13.0 kcal mol^{-1} using the CCSD(T)/6-311G** method.[104] The barrier for fulminic acid with acetylene was also investigated with CCSD(T) and G2 variants. All of the high accuracy methods give essentially the same value as the CBS-QB3 value within 0.5 kcal mol^{-1}.

4 Solvent Effects and Catalysis

4.1 Aqueous Solvation Effects in Diels–Alder and 1,3-Dipolar Cycloaddition Reactions

A fundamental principle of organic chemistry is that in comparison with less polar solvents, water may significantly accelerate or retard the rates of organic reactions involving charged species.[105] In contrast, the conventional expectation for Diels–Alder reactions involving hydrocarbon reactants is that the rate of the reaction is unaffected by solvent polarity.[106] This idea was reformulated after Breslow and co-workers discovered the surprising acceleration of neutral Diels–Alder reactions in aqueous solvents.[107] Currently accepted explanations of these results focus on acceleration of these reactions by both the hydrophobic effect,[107a] and by hydrogen bonding catalysis.[108] The hydrophobic effect accelerates the rate of the reaction by reducing the solvent accessible surface area (SASA) of the reactants during the cycloaddition process. In a normal electron demand Diels–Alder reaction, the LUMO energy of the dienophile with π-accepting groups is lowered by hydrogen bonding, leading to enhanced mixing with the HOMO of the diene. This interaction causes the transition state to be more polarized than the reactants, leading to enhanced hydrogen bonding of the solvent molecules with heteroatoms in the transition state. Preferential stabilization by this means lowers the activation energy for the reaction. Presumably, both factors are intertwined in most Diels–Alder reactions involving activated dienophiles that are accelerated by water.

Experimental[109] and theoretical[110] treatments have contributed numerous insights into the effects of aqueous solvation of Diels–Alder reactions. The results of the most recent study done by Jorgensen and co-workers lend support to earlier theoretical findings from his group and others.[111] A theoretical QM/MM approach was used to separate the contributions of enhanced hydrogen-bonding and the hydrophobic effect in Diels–Alder reactions of cyclopentadiene with acetonitrile, methyl vinyl ketone (MVK) and 1,4-naphthoquinone (Scheme 16). Monte Carlo simulations involving free energy perturbation calculations with the semi-empirical AM1 quantum mechanical method were used to generate free energy profiles for

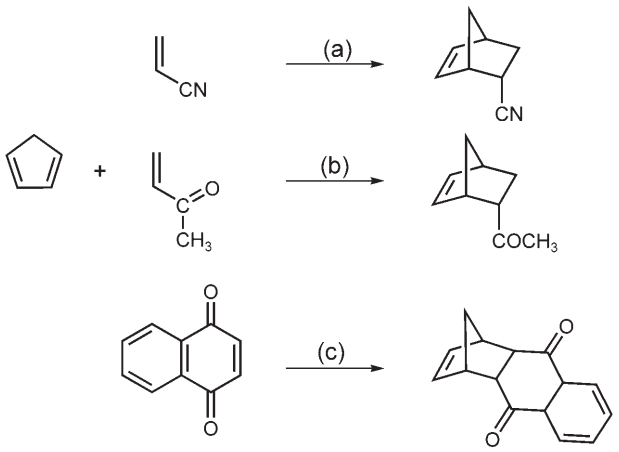

Scheme 16. Diels–Alder reactions of cyclopentadiene with (a) acetonitrile (b) methyl vinyl ketone (MVK) and (c) 1,4-naphthoquinone.

these reactions in the gas phase and in an aqueous environment of 500 water molecules.

Using this approach, the investigators found that in comparison with the gas phase, the activation energies for the reactions of cyclopentadiene with acrylonitrile, MVK and 1,4-naphthoquinone were reduced by 1.5, 2.8, and 4.4 kcal mol^{-1}, respectively, in water; these were in excellent agreement with experiment.

By evaluating the variation of the SASAs of these reactions along the reaction coordinate, the authors found that cycloaddition results in rapid reduction of the SASAs for all reactions, from the maximum value for the separated reactants, to a minimum at the transition states of these reactions. The hydrophobic effect contributes no more than 1 kcal mol^{-1} to the reduction in the activation energies of the reactions, which implies that the acceleration of these reactions in water is mostly caused by differential stabilization of the transition states by hydrogen-bonding interactions with the solvent. Water molecules formed one more hydrogen bond on average with the transition states than with reactants, because the transition states had the greatest C^+-O^- polarization.

Reactions involving non-polar substrates should be influenced by the hydrophobic effect, while in polar cases like 1,3-dipolar cycloadditions, the substrates can form strong hydrogen bonds with the solvent. Therefore, 1,3-dipolar cycloaddition reactions would be expected to be accelerated to a lesser extent in water than corresponding Diels–Alder cycloadditions.

Despite these results, Butler et al. demonstrated experimentally that the rates of some 1,3-dipolar cycloadditions can be accelerated in pure water.[112] The cycloadditions of pyridazinium-dicyanomethides (Scheme 17) with alkenes are nearly unaffected by

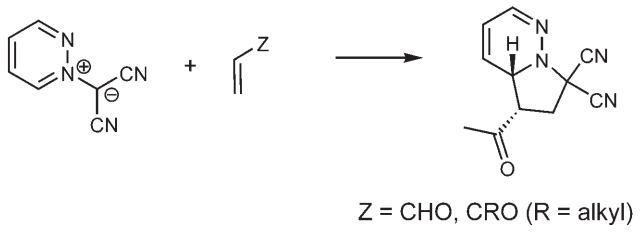

Scheme 17. 1,3-Dipolar cycloaddition reactions of pyridazinium-dicyanomethide with aldehyde and ketone substituted alkenes.

water if the alkene is substituted with ester, ether, sulfonyl, nitrile or aryl ring groups. However, the rates of reactions involving aldehyde or ketone-substituted alkenes are significantly accelerated in water, presumably because of enhanced hydrogen bonding at the transition state.

DFT calculations on the cycloadditions of pyridazinium-dicyanomethide with methyl vinyl ketone, show that the activation enthalpies are reduced by 5–7 kcal mol^{-1} by water, whereas the activation enthalpies for reactions involving methyl acrylate are only reduced by about 1 kcal mol^{-1}.

4.2 Catalysis of Hetero-Diels–Alder Cycloadditions by Non-Aqueous Solvents

The aqueous acceleration of Diels–Alder cycloadditions has been a topic of interest since being discovered by Breslow and co-workers.[107] The related hetero-Diels–Alder cycloadditions of ketones with dienes are promoted by catalysis or by pressure,[113] but the effect of solvent on these types of cycloadditions was unknown until Rawal and Huang demonstrated that hetero-Diels–Alder cycloadditions of butadiene derivatives with simple unactivated ketones are accelerated by protic polar solvents but are relatively unaffected by polar aprotic solvents.[114] Inspired by these findings, Domingo and co-workers investigated hetero-Diels–Alder reactions with DFT methods to assess the role of protic solvents in the catalysis of the hetero-Diels–Alder cycloaddition between Rawal's diene and acetone (Scheme 18).[115,116]

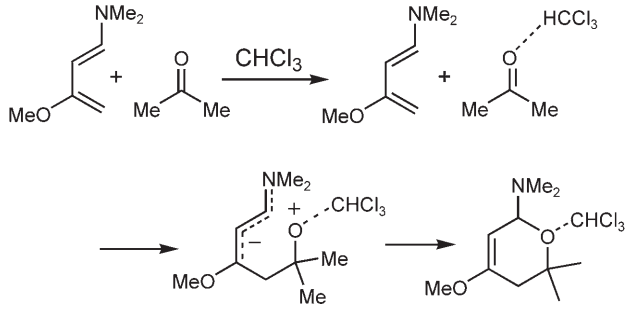

Scheme 18. Hetero-Diels–Alder cycloaddition reaction of *N,N*-dimethylamino-3-methoxy-buta-1,3-diene with acetone catalyzed by a molecule of chloroform solvent.

They found that inclusion of an explicit chloroform molecule hydrogen-bonding to the lone pairs of the carbonyl group of acetone reduces the activation enthalpy for the cycloaddition by 5 kcal mol^{-1} in comparison to the uncatalyzed reaction, and changes the mechanism of the reaction from being concerted to being a stepwise mechanism involving zwitterionic intermediates (Scheme 18).[115]

They evaluated the nature of the hydrogen-bonding interaction with a combination of natural bond orbital (NBO) theory, atoms in molecules (AIM) theory and electron localization function (ELF), and energy decomposition analysis (EDA).[116] These demonstrated that the carbonyl group of the heterodienophile becomes more polarized in the transition state of the re-

action presenting one more lone pair for hydrogen-bonding with the solvent. Therefore, even weak hydrogen-bonding solvents are capable of catalyzing these reactions, however, only those solvents which form strong hydrogen bond interactions (for example, H_2O, CH_3OH and $CHCl_3$) are capable of exploiting this polarization.

4.3 Hydrogen-Bonding Organocatalysis of Hetero-Diels–Alder Cycloadditions

Metal-free catalysis of enantioselective organic reactions has generated great interest in recent years.[117] In particular, asymmetric induction in Diels–Alder reactions is one of the most challenging aspects of this field.[118] TADDOL catalysts developed by Rawal and co-workers catalyze Diels–Alder and hetero-Diels–Alder cycloadditions that are promoted by hydrogen-bonding interactions between diol groups on the catalyst and π-acceptors of the dienophile.[119] Zhang et al. reported experimental and computational studies on the catalysis and enantioselectivities of hetero-Diels–Alder reactions organocatalyzed by TADDOL derivatives (Scheme 19).[120]

They investigated these reactions with a computational model in which Danishefsky's diene was modeled with 1,3-dimethoxybuta-1,3-diene (Scheme 19). A layered ONIOM[121] approach was used in which the reacting moieties considered most important were modeled with a high-level method, while groups that were not deemed to be as important were modeled with a lower level method. This is represented in Figure 7, in which the substrates and the core of the catalyst were modeled with B3LYP/6-31G(d) and the backbone of the catalyst was modeled with PM3.

The computational study demonstrated that various diol catalysts provide moderate to excellent acceleration of the rates of these reactions, which are in good agreement with experiment. The TADDOL promoted cycloaddition is initiated by formation of an intramolecular hydrogen-bond between the hydroxy groups of the catalyst. This increases the Lewis acidity of the free hydrogen atom belonging to one of the free hydroxy groups, which forms an intermolecular hydrogen-bond with a lone pair of the carbonyl oxygen of the heterodienophile. The transition structures for the reaction between benzaldehyde and dimethoxybutadiene organocatalyzed by TADDOL **4.1** are shown in Figure 8.

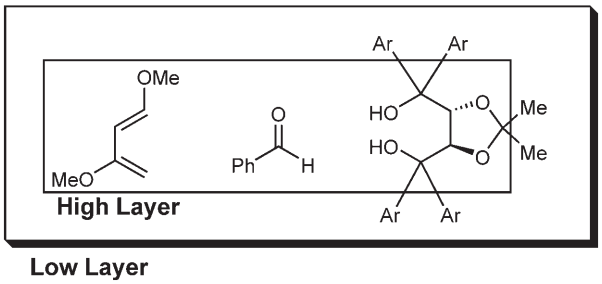

Figure 7. Layers used in ONIOM for geometry optimizations of the TADDOL-catalyzed cycloadditions of benzaldehyde and dimethoxybutadiene.

The investigators account for the stereoselectivities observed in these reactions by invoking stronger

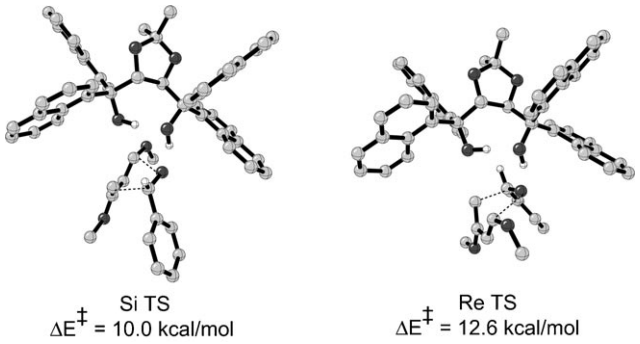

Figure 8. Transition structures for the hetero-Diels–Alder cycloaddition of benzaldehyde and 1,3-dimethoxybuta-1,3-diene catalyzed by TADDOL catalyst, **4.1**.

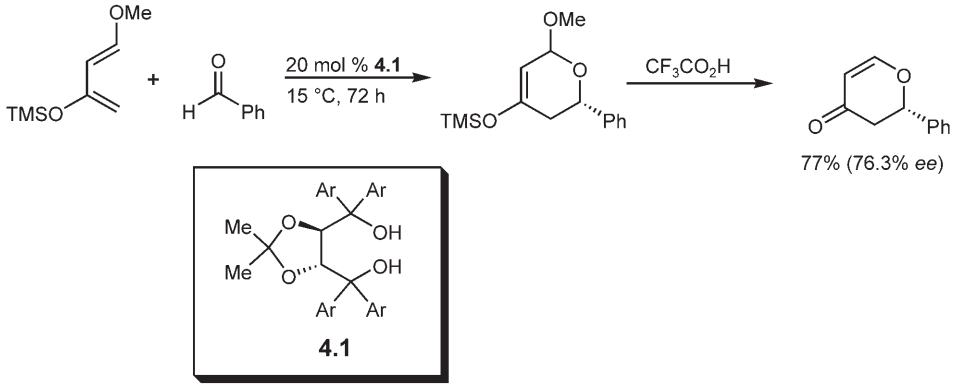

Scheme 19. Hetero-Diels–Alder reaction between Danishefsky's diene and benzaldehyde organocatalyzed by the TADDOL catalyst, **4.1**.

steric repulsion between the aryl substituents on the diol catalysts and the phenyl group of benzaldehyde in disfavored transition states. Similar considerations also account for differences in stereoselectivity obtained with various TADDOL catalysts. Enantioselectivities are high for reactions in which the aryl groups on the catalyst backbone interact strongly with the substrate in disfavored transition states.

4.3 Organocatalysis of Diels–Alder Reactions with Chiral Imidazolidinones

MacMillan and co-workers have developed amine-based organocatalysts capable of catalyzing enantioselective Diels–Alder reactions,[122,123] as well as inducing asymmetry in other types of reactions.[124]

Houk and Gordillo[125,126] used B3LYP DFT to explore the amine catalyzed Diels–Alder cycloadditions of cyclopentadiene with a variety of α,β-unsaturated aldehydes and ketones (Scheme 20). Previous studies

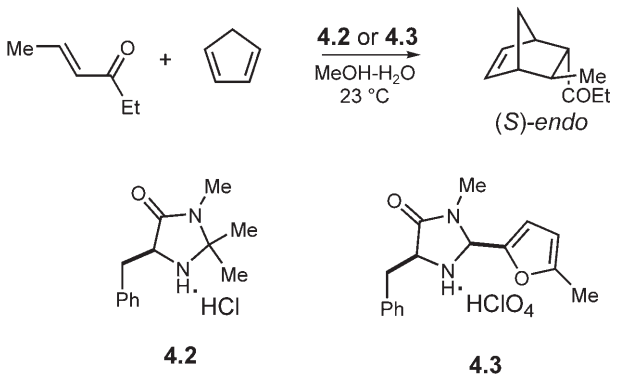

Scheme 20. Diels–Alder cycloadditions of cyclopentadiene with 4-hexen-3-one catalyzed by the chiral imidazolidinones **4.2** and **4.3**.

out of the Houk group had demonstrated that DFT can be a powerful tool to predict enantioselectivities observed experimentally in a variety of asymmetric organocatalyzed reactions.[126,127]

Iminium ions formed from condensation of amines with α,β-unsaturated aldehydes and ketones reduce the activation barriers of Diels–Alder cycloaddition reactions in comparison with uncatalyzed reactions. B3LYP calculations account for the yields and selectivities observed in cycloadditions catalyzed by the chiral imidazolidinones. For example, the formation of the iminium cation from catalyst **4.2** is slow, or does not occur, because of steric encumbrance. As a result, the background uncatalyzed reaction occurs faster than the imidazolidinone-catalyzed reaction, leading to the low yield and non-selectivity observed experimentally. In contrast, the formation of the iminium ion from catalyst **4.3** is fast, and there is a preference for attack in a sterically unencumbered fashion that leads to the high stereoselectivity observed for this reaction (Figure 9). Predicted selectivities are in excellent agreement with experiment.[125]

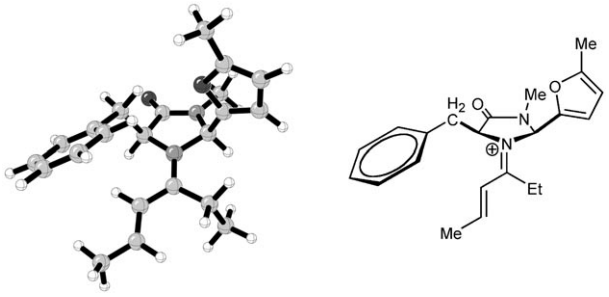

Figure 9. The iminium cation formed from condensation of chiral imidazolidinone catalyst **4.3** and 4-hexen-3-one.

4.4 Catalysis of 1,3-Dipolar Cycloaddition Reactions

The "click chemistry" methodology developed by the Sharpless group has been applied in a wide range of biological and materials chemistry contexts in the relatively short time since being introduced.[128] Arguably, the most appealing aspect of this strategy is the involvement of complementary substrates that are orthogonal to other functional groups and which participate in highly exothermic reactions.

1,3-Dipolar cycloaddition reactions of azides with terminal acetylenes (Scheme 21, **1**) and nitriles (Scheme 21, **1** and **2**), studied by Huisgen,[129,130] have been a focus of this research. The copper-catalyzed version, in which copper salts have been used to catalyze the reaction between azides and terminal acety-

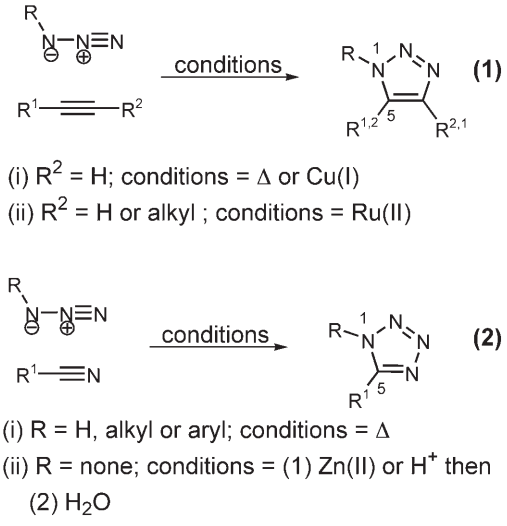

Scheme 21. Representative 1,3-dipolar cycloaddition reactions used in click chemistry.

lenes,[131] is the main reaction of click chemistry (Scheme 21, **1i**). Recently, Sharpless et al. reported ruthenium-catalyzed cycloadditions between organic azides and monosubstituted, as well as disubstituted alkynes, that form 1,5-disubstituted 1,2,3-triazoles and 1,4,5-trisubstituted 1,2,3-triazoles, respectively (Scheme 21, **1ii**).[132] Catalysis of reactions between organic nitriles and azide salts by magnesium,[133] zinc[134] and proton[135] (Scheme 21, **2ii**) sources have also been studied.

While the mechanisms of the uncatalyzed versions of these reactions are well established,[136] the mechanisms by which adducts are formed by catalysis are less evident. The Scripps group, in an effort to elucidate the mechanisms of the uncatalyzed and catalyzed versions of these 1,3-dipolar cycloadditions, has relied on DFT methods to investigate the several possibilities involved in each of the acid-, zinc- and copper-catalyzed processes.

DFT calculations on the uncatalyzed reactions between nitriles and organic azides reveal that the reaction proceeds by a concerted [3+2] mechanism.[135] Calculations predict that the barriers for reactions of methyl azide with electron-deficient and electron-rich nitriles range from 18 kcal mol^{-1} to 35 kcal mol^{-1}, respectively, and predict the preference for the formation of 1,5-disubstituted adducts over 2,5-disubstituted adducts, in excellent agreement with experiment.

Three mechanisms were considered for fast formation of 1-tetrazoles from reactions involving anionic azides and nitriles: the uncatalyzed process, and Lewis acid catalysis by proton sources,[135] and zinc salts.[137] Only mechanisms identified as being most probable are presented here.

The barriers for the uncatalyzed reactions of the azide anion with electron-rich nitriles are almost identical to the barriers for 1,3-dipolar cycloadditions involving neutral methyl azide. However, the activation barriers of reactions of the azide anion with electron-deficient nitriles are lowered by as much as 13 kcal mol^{-1} in comparison with the organic azide. The most likely mechanism for acid catalyzed cycloaddition of azide anion to organic nitriles involves activation of the nitrile by proton sources proceeding from the eight-membered TS shown in Scheme 22, leading to the formation of intermediate P. Zinc catalysis is similar, but is predicted to involve prior activation, by zinc, of a bound nitrile molecule, followed by cycloaddition with a free azide anion.[137]

Two possible mechanisms for the copper-catalyzed reactions of organic azides with terminal acetylenes[138] may involve either concerted addition of the azide to the η-complexed alkyne, or concerted addition of the azide to the copper-acetylide complex (Scheme 23a and b, respectively). DFT calculations reveal that the activation enthalpies for these concerted processes are comparable to activation enthalpies for the uncatalyzed, concerted variant. Alternatively, the mechanism may involve stepwise addition of the azide to the copper-acetylide complex followed by attack of the distal nitrogen to C2 of the acetylide resulting in the formation of a 6-membered metallacycle (Scheme 23c**)**. Ring contraction results in the exothermic formation of the 5-membered triazolyl copper complex, that affords the 1,2,3 triazole after protonation. The activation enthalpy for the rate-determining step of this process, formation of the 6-membered metallacycle, is 11 kcal mol^{-1} lower than the barrier for the uncatalyzed cycloaddition, corresponding to a 10^5 acceleration in the rate of the reaction.

The stepwise mechanism adequately accounts for formation of 1,4-disubstituted adducts from the azide. Furthermore, investigations demonstrate that copper-catalyzed cycloadditions of acetylenes with other dipolarophiles, such as isoxazoles, may also involve this stepwise process.[138]

The ruthenium-catalyzed reactions of azides with disubstituted alkynes (Scheme 21, **1ii**),[132] illustrates that catalysis of 1,3-dipolar cycloadditions may not only involve coordination of Lewis acids to the nitrogen atom of the nitrile, or formation of metal-acetylide complexes from terminal acetylenes as general mechanisms. Evidently, while copper-acetylides are preformed from terminal alkynes, formation of metallo-alkyne η-complexes may be the preferred mechanism in ruthenium catalyzed cycloadditions. These findings expand the scope of reactants and catalysts that may be used in these 1,3-dipolar cycloaddition reactions, and suggest new frontiers in the catalysis of 1,3-dipolar cycloadditions.

In connection with the results from the Scripps group, Kuznetsov et al. reported computational inves-

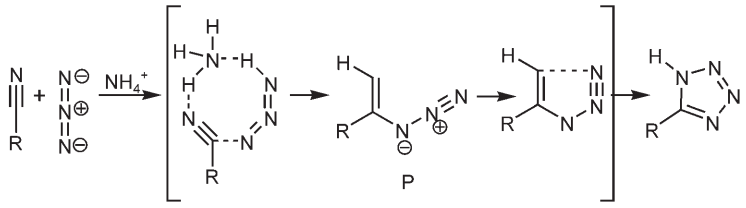

Scheme 22. Mechanism for formation of 5-tetrazoles from anionic azides and nitriles catalyzed by the ammonium cation, as predicted by B3LYP.

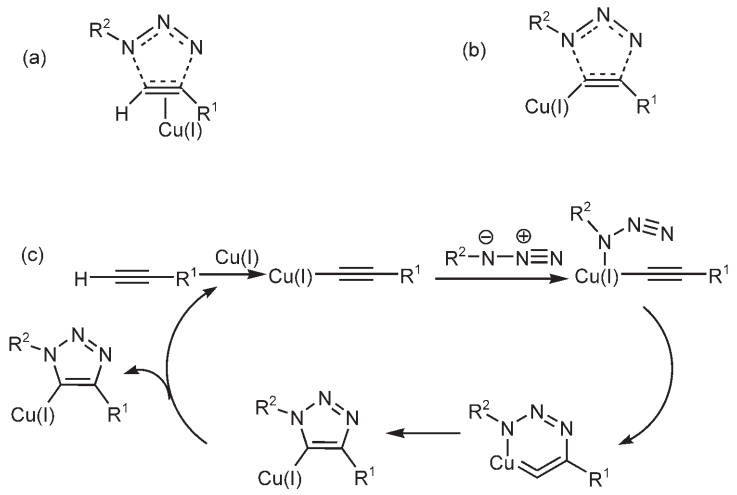

Scheme 23. Possible mechanisms in the copper-catalyzed 1,3-dipolar cycloadditions of organic azides and terminal acetylenes.

tigations on reactant activation in Pt(II)- and Pt(IV)-catalyzed cycloadditions of cyclic nitrones with nitriles to form oxadiazoline cycloadducts (Scheme 24). The

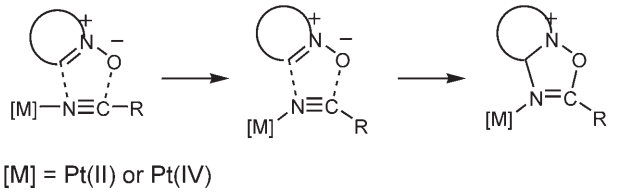

[M] = Pt(II) or Pt(IV)

Scheme 24. Platinum-catalyzed 1,3-dipolar cycloadditions of activated nitrones with organic nitriles.

investigators found that activation enthalpies for cycloadditions of Pt-bound nitriles with nitrones were considerably reduced in comparison with the corresponding uncatalyzed reactions.[139]

5 Conclusion

This review has discussed the application and performance of conceptual theories and quantitative quantum mechanical methods to the study of mechanism, reactivity, and selectivity of 1,3-dipolar and Diels–Alder cycloadditions. Conceptual DFT can be effective at understanding the nucleophilicity and electrophilicity of reactants and atomic sites of molecules, and when the HSAB principle is applied, leads to prediction of regiochemistry. The applications of configuration mixing models in cycloadditions have been discussed. The applications of recently developed highly accurate quantum mechanical methods such as CBS-QB3, G3, G2MS, G2MP2 all give essentially the same values for barrier heights and reaction energetics for cycloadditions. DFT and *ab initio* methods vary in their ability accurately predict barriers and reaction energetics, depending on the test set used. Applications of computations to the study of solvation effects, organocatalysis and metal catalysis on the rates of 1,3-dipolar and Diels–Alder cycloadditions conclude the review.

References

[1] a) W. Carruthers, *Cycloaddition Reactions in Organic Synthesis*, Pergamon, Oxford, **1990**; b) *Synthetic Applications of 1,3-Dipolar Cycloaddition Chemistry Toward Heterocycles and Natural Products*, (Eds.: A. Padwa, W. H. Pearson), John Wiley & Sons, New York, **2002**.

[2] a) R. G. Parr, W. Yang, *Density-Functional Theory of Atoms and Molecules*, Oxford, **1989**; b) *Recent Advances in Density Functional Methods*, Parts. I and II, (Ed.: D. P. Chong), World Scientific, Singapore, **1997**; c) *Recent Advances in Density Functional Methods*, Part. III, (Eds.: V. Barone, A. Bencini), World Scientific, Singapore, **1999** and all references cited therein pertaining to density functional theory.

[3] For a review of mechanistic, regio-, stereo-, and enantioselectivity issues and a history of the debates that have occurred for cycloadditions, see: K. N. Houk, J. González, Y. Li, *Acc. Chem. Res.* **1995**, *28*, 81–90.

[4] a) K. Fukui, H. Fujimoto, *Bull. Chem. Soc. Jpn.* **1967**, *40*, 2018; b) K. Fukui, H. Fujimoto, *Bull. Chem. Soc. Jpn.* **1969**, *42*, 3399; c) K. Fukui, *Fortschr. Chem. Forsch.* **1970**, *15*, 1; d) K. Fukui, *Acc. Chem. Res.* **1971**, *4*, 57; e) K. N. Houk, *Acc. Chem. Res.* **1975**, *8*, 361; for reviews, see: f) K. N. Houk, in: *Pericyclic Reactions*, Vol. 2, (Eds.: A. P. Marchand; R. E. Lehr), Academic Press, New York, **1977**, p. 181; g) K. Fukui, *Angew. Chem. Int. Ed. Engl.* **1982**, *21*, 801.

[5] K. N. Houk, K. Yamaguchi, in: *1,3-Dipolar Cycloaddition Chemistry*, Vol. 2, (Ed.: A. Padwa), John Wiley & Sons, New York, **1984**, Chapter 13.

[6] a) P. V. Alston, R. M. Ottenbrite, D. D. Shillady, *J. Org. Chem.* **1973**, *38*, 4075; b) P. V. Alston, R. M. Ottenbrite, *J. Org. Chem.* **1975**, *40*, 1111; c) P. V. Alston, R. M. Ottenbrite, T. Cohen, *J. Org. Chem.* **1978**, *43*, 1864; d) T. Cohen, R. J. Ruffner, D. W. Shull, W. M. Daniewski, R. M. Ottenbrite, P. V. Alston, *J. Org. Chem.* **1978**, 43, 4052; for a review, see: e) D. Ginsburg, *Tetrahedron* **1983**, *39*, 2095.

[7] S. D. Kahn, C. F. Pau, L. E. Overman, W. J. Hehre, *J. Am. Chem. Soc.* **1986**, *108*, 7381.

[8] B. R. Ussing, C. Hang, D. A. Singleton, *J. Am. Chem. Soc.* **2006**, *128*, 7594.

[9] C. Spino, H. Rezaei, Y. L. Dory, *J. Org. Chem.* **2004**, *69*, 757.

[10] P. Geerlings, F. De Proft, W. Langenaeker *Chem. Rev.* **2003**, *103*, 1793–1873.

[11] F. Méndez, M. A. Garcia-Garibay, *J. Org. Chem.* **1999**, *64*, 7061–7066.

[12] B. Safi, K. Choho, P. Geerlings, *J. Phys. Chem. A* **2001**, *105*, 591–601.

[13] F. Méndez, J. L. Gázquez, *J. Am. Chem. Soc.* **1994**, *116*, 9298–9301.

[14] M. Boiani, H. Cerecetto, M. González, O. E. Piro, E. E. Castellano, *J. Phys. Chem. A* **2004**, *108*, 11241–11248.

[15] B. Safi, J. Mertens, F. De Proft, R. Alberto, P. Geerlings, *J. Phys. Chem. A* **2005**, *109*, 1944–1951.

[16] G. Roos, S. Loverix, F. De Proft, L. Wyns, P. Geerlings, *J. Phys. Chem. A* **2003**, *107*, 6828–6836.

[17] a) P. Geerlings, F. De Proft, *Int. J. Quantum. Chem.* **2000**, *80*, 227–235; NCO addition to acetylenes; b) H.-T. Chen, J.-J. Ho, *J. Phys. Chem. A* **2003**, *107*, 7643–7649; isocyanide to dipolarophiles; c) A. K. Chandra, P. Geerlings, M. T. Nguyen, *J. Org. Chem.* **1997**, *62*, 6417–6419.

[18] a) R. G. Pearson, *J. Am. Chem. Soc.* **1963**, *85*, 3533–3539; b) *Hard and Soft Acids and Bases*, (Ed.: R. G. Pearson), Dowden, Hutchinson and Ross, Inc., Stroudsburg, Pennsylvania, **1973**; c) H. Fujimoto, K. Fukui, in: *Chemical Reactivity and Reaction Paths*, (Ed.: G. Klopman), Wiley-Interscience Publication, New York, **1974**, pp. 23–54; d) H. G. Klopman, in: *Chemical Reactivity and Reaction Paths*, (Ed.: G. Klopman), Wiley-Interscience Publication, New York, **1974**, pp. 55–71.

[19] a) R. G. Pearson, in: *Theoretical Models of Chemical Bonding - Part 2 the Concept of the Chemical Bond*, (Ed.: Z. B. Maksic), Springer-Verlag, Berlin Heidelberg, **1990**; b) K. R. S. Chandrakumar, S. Pal, *Int. J. Mol. Sci.* **2002**, *3*, 324–337; c) P. K. Chatttaraj, H. Lee, R. G. Parr, *J. Am. Chem. Soc.* **1991**, *113*, 1855–1856; d) R. G. Parr, P. K. Chatttaraj, *J. Am. Chem. Soc.* **1991**, *113*, 1854–1855; e) R. G. Parr, W. Yang, *J. Am. Chem. Soc.* **1984**, *106*, 4049–4050; f) J. L. Gázquez, F. Méndez, *J. Phys. Chem.* **1994**, *98*, 4591–4593; g) P. Geerlings, F. De Proft, W. Langenaeker, *Chem. Rev.* **2003**, *103*, 1793–1873.

[20] a) R. G. Parr, J. L. Gázquez, *J. Phys. Chem.* **1993**, *97*, 3939–3940; b) F. Méndez, J. L. Gázquez, *J. Am. Chem. Soc.* **1994**, *116*, 9298–9301.

[21] Y. Li, J. N. S. Evans, *J. Am. Chem. Soc.* **1995**, *117*, 7756–7759.

[22] a) A. K. Chandra, T. Uchimaru, M. T. Nguyen, *J. Chem. Soc., Perkin Trans. 2* **1999**, 2117–2121; b) J. Korchowiec, A. K. Chandra, T. Uchimaru, *J. Mol. Struct. THEOCHEM*, **2001**, *572*, 193–202.

[23] L. T. Nguyen, F. De Proft, V. L. Dao, M. T. Nguyen, P. Geerlings, *J. Phys. Org. Chem.* **2003**, *16*, 615–625.

[24] a) A. K. Chandra, M. T. Nguyen, *J. Phys. Chem. A* **1998**, *102*, 6181–6185; b) A. K. Chandra, M. T. Nguyen, *J. Comp. Chem.* **1998**, *19*, 195–202.

[25] L. Nyulázi, P. Várnai, W. Eisfeld, M. Regitz, *J. Comp. Chem.* **1997**, *18*, 609–616.

[26] a) S. Damoun, G. Van de Woude, F. Méndez, P. Geerlings, *J. Phys. Chem. A* **1997**, *101*, 886–893; b) Y. Cong, Z-Z. Yang, C-S. Wang, X-C. Liu, X-H. Bao, *Chem. Phys. Lett.* **2002**, *357*, 59–64.

[27] O. Eisenstein, J. M. Lefour, N. T. Anh, R. F. Hudson, *Tetrahedron* **1977**, *33*, 523.

[28] R. Herrera, A. Nagarajan, M. A. Morales, F. Méndez, H. A. Jiménez-Vázquez, L. G. Zepeda, J. Tamariz, *J. Org. Chem.* **2001**, *66*, 1252–1263.

[29] a) G. B. Mullen, G. A. Bennett, P. A. Swift, D. M. Marinyak, P. G. Dormer, V. St. Georgiev, *Liebigs Ann. Chem.* **1990**, 105; b) P. N. Confalone, E. M. Huie, *Org. React.* **1988**, *36*, 1; c) A. Z. Bimanad, K. N. Houk, *Tetrahedron Lett.* **1983**, *24*, 435.

[30] F. Méndez, J. Tamariz, P. Geerlings, *J. Phys. Chem. A* **1998**, *102*, 6292–6296.

[31] A. Ponti, *J. Phys. Chem. A* **2000**, *104*, 8843–8846.

[32] A. Ponti, G. Molteni, *J. Org. Chem.* **2001**, *66*, 5252–5255.

[33] G. Molteni, A. Ponti, *Chem. Eur. J.* **2003**, *9*, 2770–2774.

[34] A. Ponti, G. Molteni, *Chem. Eur. J.* **2006**, *12*, 1156–1161.

[35] R. Huisgen, R. Sustmann, G. Wallbillich *Chem. Ber.* **1967**, *100*, 1786–1801.

[36] A. T. Maynard, M. Huang, W. G. Rice, D. G. Covell, *Proc. Natl. Acad. Sci.* **1998**, *95*, 11578–11583.

[37] R. G. Parr, L. v. Szentpály, S. Liu, *J. Am. Chem. Soc.* **1999**, *121*, 1922–1924.

[38] P. K. Chattaraj, U. Sarkar, D. R. Roy, *Chem. Rev.* **2006**, *106*, 2065–2091.

[39] P. Pérez, L. R. Domingo, M. J. Aurell, R. Contreras, *Tetrahedron* **2003**, *59*, 3117–3125.

[40] P. Pérez, L. R. Domingo, M. J. Aurell, R. Contreras, *Tetrahedron* **2002**, *58*, 4417–4423.

[41] L. R. Domingo, M. J. Aurell, P. Pérez, R. Contreras, *J. Org. Chem.* **2003**, *68*, 3884–3890.

[42] L. R. Domingo, M. T. Picher, P. Arroyo, *Eur. J. Org. Chem.* **2006**, 2570–2580.

[43] L. R. Domingo, M. Arnó, R. Contreras, P. Pérez, *J. Phys. Chem. A* **2002**, *106*, 952–961.

[44] J. A. Sáez, M. Arnó, L. R. Domingo, *Tetrahedron* **2003**, *59*, 9167–9171.

[45] L. R. Domingo, A. Asensio, P. Arroyo, *J. Phys. Org. Chem.* **2002**, *15*, 660–666.

[46] C. N. Alves, A. S. Carneiro, J. Andrés, L. R. Domingo, *Tetrahedron* **2006**, *62*, 5502–5509.
[47] L. R. Domingo, *Tetrahedron* **2002**, *58*, 3765–3774.
[48] M. Arnó, M. T. Picher, L. R. Domingo, J. Andrés, *Chem. Eur. J.* **2004**, *10*, 4742–4749.
[49] J. L. G. Ruano, A. Fraile, G. González, M. R. Martín, F. R. Clemente, R. Gordillo, *J. Org. Chem.* **2003**, *68*, 6522–6534.
[50] S. Noorizadeh, H. Maihami, *J. Mol. Struct. THEOCHEM*, **2006**, *763*, 133–144.
[51] a) L. R. Domingo, M. J. Aurell, P. Pérez, R. Contreras, *J. Phys. Chem. A* **2002**, *106*, 6871; b) L. R. Domingo, M. J. Aurrell, *J. Org. Chem.* **2002**, *67*, 959–965; c) S. Azzouzi, M. E. Messaoudi, M. Esseffar, R. Jalal, F. H. Cano, M. del C. Apreda-Rojas, L. R. Domingo, *J. Phys. Org. Chem.* **2005**, *18*, 522–528.
[52] M. J. Aurell, L. R. Domingo, P. Pérez, R. Contreras, *Tetrahedron* **2004**, *60*, 11503–11509.
[53] P. Merino, J. Revuelta, R. Tejero, U. Chiacchio, A. Rescifina, G. Romeo, *Tetrahedron* **2003**, *59*, 3581–3592.
[54] A. Corsaro, V. Pistarà, A. Rescifina, A. Piperno, M. A. Chiacchio, G. Romero, *Tetrahedron* **2004**, *60*, 6443–6451.
[55] P. Arroyo, M. T. Picher, L. R. Domingo, F. Terrier, *Tetrahedron* **2005**, *61*, 7359–7365; S. Kurbatov, R. Goumont, S. Lakhdar, J. Marrot, F. Terrier, *Tetrahedron* **2005**, *61*, 8167–8176.
[56] G. Gayatri, G. N. Sastry, *J. Chem. Sci.* **2005**, *117*, 573–582.
[57] A. Pross, S. S. Shaik, *Acc. Chem. Res.* **1983**, *16*, 363–370.
[58] M-D. Su, H-Y, Liao, W-S. Chung, S-Y. Chu, *J. Org. Chem.* **1999**, *64*, 6710–6716.
[59] H-Y. Liao, M-D. Su, W-S. Chung, S-Y. Chu, *Inter. J. Quantum Chemistry* **2001**, *83*, 318–323.
[60] M. T. Nguyen, A. K. Chandra, S. Sakai, K. Morokuma, *J. Org. Chem.* **1999**, *64*, 65–69.
[61] S. Sakai, M. T. Nguyen, *J. Phys. Chem. A* **2004**, *108*, 9169–9179.
[62] S. Sakai, M. T. Nguyen, *J. Phys. Chem. A* **2000**, *104*, 922–927.
[63] P. B. Karadakov, D. L. Cooper, J. Garratt, *Theor. Chem. Acc.* **1998**, *100*, 222–229.
[64] a) J. J. Blavins, P. B. Karadakov, D. L. Cooper, *J. Phys. Chem. A* **2003**, *107*, 2548–2559; b) J. J. Blavins, P. B. Karadakov, D. L. Cooper, *J. Org. Chem.* **2001**, *66*, 4285–4292.
[65] P. B. Karadakov, D. L. Cooper, J. Garratt, *J. Am. Chem. Soc.* **1998**, *120*, 3975–3981.
[66] R. D. Harcourt, A. Schulz, *J. Phys. Chem. A* **2000**, *104*, 6510–6516.
[67] a) M. T. Nguyen, A. K. Chandra, T. Uchimaru, S. Sakai, *J. Phys. Chem. A* **2001**, *105*, 10943–1094; b) R. D. Harcourt, *J. Phys. Chem. A* **2001**, *105*, 10947–10948.
[68] V. Polo, J. Andres, R. Castillo, S. Berski, B. Silvi, *Chem. Eur. J.* **2004**, *10*, 5165–5172.
[69] S. Berski, J. Andrés, B. Silvi, L. R. Domingo, *J. Phys. Chem. A* **2003**, *107*, 6014–6024.
[70] R. C. Mawhinney, H. M. Muchall, G. H. Peslherbe, *Chem. Commun.* **2004**, 1862–1863.
[71] F. Cargoni, G. Molteni, D. L. Cooper, M. Raimondi, A. Ponti, *Chem. Commun.* **2006**, 1030–10323.
[72] *Quantum-Mechanical Prediction of Thermochemical Data*, Vol. 22, (Ed.; J. Cioslowski), Kluwer Academic Publishers, Boston, MA, **2001**, pp. 1–245.
[73] a) G-series: J. A. Pople, M. Head-Gordon, D. J. Fox, K. Raghavachari, L. A. Curtiss, *J. Chem. Phys.* **1989**, *90*, 5622–5629; b) L. A. Curtiss, C. Jones, G. W. Trucks, K. Raghavachari, J. A. Pople, *J. Chem. Phys.* **1990**, *93*, 2537–2545; c) L. A. Curtiss, G. W. Trucks, K. Raghavachari, J. A. Pople, *J. Chem. Phys.* **1991**, *94*, 7221–7230; d) L. A. Curtiss, K. Raghavachari, P. C. Redfern, V. Rassolov, J. A. Pople, *J. Chem. Phys.* **1998**, *109*, 7764–7776; e) CBS-series: J. A. Montgomery, M. J. Frisch, J. W. Ochterski, G. A. Petersson, *J. Chem. Phys.* **1999**, *110*, 2822–2827; f) M. R. Nyden, G. A. Petersson, *J. Chem. Phys.* **1981**, *75*, 1843–1862; g) M. A. Al-Laham, G. A. Petersson, *J. Chem. Phys.* **1991**, *94*, 6081–6090; h) G. A. Petersson, T. G. Tensfeldt, J. A. Montgomery, *J. Chem. Phys.* **1991**, *94*, 6091–6101; i) G. A. Petersson, D. K. Malick, W. G. Wilson, J. W. Ochterski, J. A. Montgomery, M. J. Frisch, *J. Chem. Phys.* **1998**, *109*, 10570–10579; j) J. A. Montgomery, M. J. Frisch, J. W. Ochterski, G. A. Petersson, *J. Chem. Phys.* **2000**, *112*, 6532–6542; k) W-series: J. M. L. Martin, G. Oliveria, *J. Chem. Phys.* **1999**, *111*, 1843–1856.
[74] See ref.[2] for a general DFT review.
[75] Density functional calculations have become such a common place that the vast majority of first principles or quantum mechanical studies use DFT.
[76] a) Y. Feng, L. Liu, J-T. Wang, H. Huang, Q-X. Guo, *J. Chem. Inf. Comput. Sci.* **2003**, *43*, 2005–2013; b) X-J. Qi, Y. Feng, L. Liu, Q-X. Guo, *Chin. J. Chem.* **2005**, *23*, 194–199; c) T. M. Gilbert, *J. Phys. Chem. A* **2004**, *108*, 2550–2554; d) D. Kaur, R. P. Kaur, *J. Mol. Struct. THEOCHEM*, **2005**, *757*, 53–59; e) F. Agapito, B. J. Costa Cabral, J. A. Martinho Simoes, *J. Mol. Struct. THEOCHEM*, **2005**, *719*, 109–114; f) J. Cioslowski, G. Liu, D. Moncrieff, *J. Am. Chem. Soc.* **1997**, *119*, 11452–11457.
[77] a) D. J. Henry, C. J. Parkinson, L. Radom, *J. Phys. Chem. A* **2002**, *106*, 7927–7936; b) P. C. Redfern, P. Zapol, L. A. Curtiss, K. Raghavachari, *J. Phys. Chem. A* **2000**, *104*, 5850–5854.
[78] M. H. Liu, C. Chen, *J. Comput. Chem.* **2006**, *27*, 537–544.
[79] M. Swart, F. M. Bickelhaupt, *J. Chem. Theory Comput.* **2006**, *2*, 281–287.
[80] M. L. Coote, *J. Phys. Chem. A* **2004**, *108*, 3865–3872.
[81] G. P. F. Wood, D. J. Henry, L. Radom, *J. Phys. Chem. A* **2003**, *107*, 7985–7990; R. Gómez-Balderas, M. L. Coote, D. J. Henry, L. Radom, *J. Phys. Chem. A* **2004**, *108*, 2874–2883; D. J. Henry, C. J. Parkinson, P. M. Mayer, L. Radom, *J. Phys. Chem. A* **2001**, *105*, 6750–6756.
[82] a) Y. Zhao, D. G. Truhlar, *J. Chem. Theory Comput.* **2006**, *2*, 1009–1018; b) Y. Zhao, O. Tishchenko, D. G. Truhlar, *J. Phys. Chem. B* **2005**, *109*, 19046–19051; c) Y. Zhao, D. G. Truhlar, *J. Phys. Chem. A* **2005**, *109*, 4209–4212; d) Y. Zhao, D. G. Truhlar, *Phys. Chem. Chem. Phys.* **2005**, *7*, 2701–2705; e) Y. Zhao, D. G.

Truhlar, *J. Chem. Theory Comput.* **2005**, *1*, 415–432; f) Y. Zhao, D. G. Truhlar, *J. Phys. Chem. A* **2004**, *108*, 6908–6918; g) J. Cerny, P. Hobza, *Phys. Chem. Chem. Phys.* **2005**, *7*, 1624–1626; h) X. Zu, W. A. Goddard, III, *J. Phys. Chem. A* **2004**, *108*, 2305–2313; i) E. R. Johnson, G. A. DiLabio, *Chem. Phys. Lett.* **2006**, *419*, 333–339; j) A. Müller, M. Losada, S. Leutwyler, *J. Phys. Chem. A* **2004**, *108*, 157–165.

[83] a) S. Parthiban, G. de Oliveria, J. M. L. Martin, *J. Phys. Chem. A* **2001**, *105*, 895–904; b) Y. Ren, J. L. Wolk, S. Hoz, *Int. J. Mass Spec.* **2002**, *221*, 59–65.

[84] S. Sakai, *Internet Electronic J. Mol. Design* **2002**, 1, 462–466.

[85] T. C. Dinadayalane, R. Vijaya, A. Smitha, G. N. Sastry, *J. Phys. Chem. A* **2002**, *106*, 1627–1633.

[86] J. Baker, P. Pulay, *J. Chem. Phys.* **2002**, *117*, 1441–1449.

[87] a) B. J. Lynch, D. G. Truhlar, *J. Phys. Chem. A* **2001**, *105*, 2936–2941; b) Y. Zhao, B. J. Lynch, D. G. Truhlar, *J. Phys. Chem. A* **2004**, *108*, 2715–2719.

[88] a) B. Amekraz, J. Tortajada, J. P. Morizur, A. I. González, O. Mó, M. Yáñez, *J. Mol. Struct. THEOCHEM*, **1996**, *371*, 313–324; b) first transition metal row: O. Salomon, M. Reiher, B. A. Hess, *J. Chem. Phys.* **2002**, *117*, 4729–4737; c) transition metal compounds: T. Strassner, M. A. Taige, *J. Chem. Theory Comput.* **2005**, *1*, 848–855; d) oxidative addition: G. T. de Jong, F. M. Bickelhaupt, *J. Chem. Theory Comput.* **2006**, *2*, 322–335; e) G. T. de Jong, F. M. Bickelhaupt, *J. Phys. Chem. A* **2005**, *109*, 9685–9699; f) G. T. de Jong, D. P. Geerke, A. Diefenbach, F. M. Bickelhaupt, *Chem. Phys.* **2005**, *313*, 261–270; g) G. T. de Jong, D. P. Geerke, A. Diefenbach, M. Solà, F. M. Bickelhaupt, *J. Comput. Chem.* **2005**, *26*, 1006–1020; h) excitation energies: M. C. Holthausen, *J. Comput. Chem.* **2005**, *26*, 1505–1518; i) iron spin states: R. J. Deeth, N. Fey, *J. Comput. Chem.* **2004**, *25*, 1840–1848; j) late transition metal reactions: M. M. Quintal, A. Karton, M. A. Iron, A. D. Boese, J. M. L. Martin, *J. Phys. Chem. A* **2006**, *110*, 709–716; k) manganese complexes: M. Lundberg, P. E. M. Siegbahn, *J. Comput. Chem.* **2005**, *26*, 661–667; l) metal aqua ions: F. P. Rotzinger, *J. Phys. Chem. B* **2005**, *109*, 1510–1527; m) mercury(IV) complexes: S. Riedel, M. Straka, M. Kaupp, *Phys. Chem. Chem. Phys.* **2004**, *6*, 1122–1127; n) aluminum compounds: B. G. Willis, K. F. Jensen, *J. Phys. Chem. A* **1998**, *102*, 2613–2623; o) general benchmark: N. E. Schultz, Y. Zhao, D. G. Truhlar, *J. Phys. Chem. A* **2005**, *109*, 11127–11143.

[89] a) G. R. Hutchinson, M . A. Ratner, T. J. Marks, *J. Phys. Chem. A* **2002**, *106*, 10596–10605; b) S. A. Zygmunt, R. M. Mueller, L. A. Curtiss, L. E. Iton, *J. Mol. Struct. THEOCHEM*, **1998**, *430*, 9–16; c) B. S. Jursic, *J. Mol. Struct. THEOCHEM*, **2000**, *499*, 137–140.

[90] S. Andersson, M. Grüning, *J. Phys. Chem. A* **2004**, *108*, 7621–7636.

[91] V. Guner, K. S. Khuong, A. G. Leach, P. S. Lee, M. D. Bartberger, K. N. Houk, *J. Phys. Chem. A* **2003**, *107*, 11445–11459 (Reactions 10 and 11 were not used in the statistical benchmark because of the significant errors associated with the experimental measurements).

[92] V. A. Guner, K. S. Khuong, K. N. Houk, A. Chuma, P. Pulay, *J. Phys. Chem. A* **2004**, *108*, 2959–2965.

[93] The hybrid DFT methods B3LYP, MPW1K, and O3LYP use empirically-determined percentages of Hartree–Fock exact exchange along with density functionals to recover exchange and correlation energies. B3LYP was parameterized against atomization and atomic energies, ionization potential, and proton affinities form the G1 test set (A. D. Becke, *J. Chem. Phys.* **1993**, *98*, 5648–5652; P. J. Stephens, F. J. Devlin, C. F. Chabalowski, M. J. Frisch, *J. Chem. Phys.* **1994**, *98*, 11623–11627). MPW1K was designed by Truhlar and co-workers specifically for barrier heights (B. J. Lynch, P. L. Fast, M. Harris, D. G. Truhlar, *J. Phys. Chem. A* **2000**, *104*, 4811–4815). O3LYP is similar to B3LYP, except the local exchange functional was designed to have an increased flexibility to deal with the inseparability of DFT exchange and non-dynamic correlation effects (N. C. Handy, A. J. Cohen, *J. Chem. Phys.* **1998**, *108*, 2545; W. M. Hoe, A. J. Cohen, N. C. Handy, *Chem. Phys. Lett.* **2001**, *341*, 319). The very accurate CBS-QB3 method is a five-step method starting with a B3LYP geometry and frequency calculation followed by CCSD(T), MP4SDQ, and MP2 single-point calculations and extrapolation to a complete basis set. The CASPT2 balances nondynamical (multi-configuration) and dynamical electron correlation with a second-order perturbation treatment [K. Andersson, P. Malmqvist, B. O. Roos, *J. Chem. Phys.* **1992**, *96*, 1218–1226; K. Andersson, B. O. Roos, in: *Modern Electronic Structure Theory*, (Ed.; D. R. Yarkony), World Scientific, Singapore, **1995**, p 55].

[94] There are a number of recent investigations that have shown B3LYP is incapable of correctly accounting for the correlation energy in larger hydrocarbon systems. Beyond the *ad hoc* explanation of strain, it may well be the problem with describing dispersion forces and medium range electron correlation effects: S. Grimme, *Angew. Chem. Int. Ed.* **2006**, *45*, 4460; M. D. Wodrich, C. Corminboeuf, P. von R. Schleyer, *Org. Lett.* **2006**, *8*, 3631–3634; P. R. Schreiner, A. A. Fokin, R. A. Pascal, A. de Meijere, *Org. Lett.* **2006**, *8*, 3635–3638.

[95] These methods use a CCSD(T) calculation with a small basis set and two MP2 calculations with large basis sets to estimate the basis set effect: a) R. D. J. Froese, S. Humbel, M. Svensson, K. Morokuma, *J. Phys. Chem. A* **1997**, *101*, 227–233; b) R. D. J. Froese, J. M. Coxon, S. C. West K. Morokuma, *J. Org. Chem.* **1997**, *62*, 6991–6996.

[96] R. C. Dinadayalane, R. Vijaya, A. Smitha, G. N. Sastry, *J. Phys. Chem. A* **2002**, *106*, 1627–1633.

[97] T. P. M. Goumans, A. W. Ehlers, K. Lammertsma, E-U. Würthwein, S. Grimme, *Chem. Eur. J.* **2004**, *10*, 6468–6475.

[98] S. Grimme, *J. Chem. Phys.* **2003**, *118*, 9095–9102. The SCS-MP2 method scales the electron correlation energy by 6/5 and 1/3 (values based on QCISD(T) calculations) for spin-antiparallel and spin-parallel correlation energies to correct for the overcorrection of MP2 of correlation energy.

[99] G. O. Jones, V. A. Guner, K. N. Houk, *J. Phys. Chem. A* **2006**, *110*, 1216–1224.
[100] a) J. W. Hehre, *A Guide to Moleuclar Mechanics and Quantum Chemical Calculations*, Wavefunction, Inc., Irvine, CA, **2003**, p. 304; b) L. R. Domingo, M. J. Aurell, P. Pérez, R. Contreras, *J. Org. Chem.* **2003**, *68*, 3884–3890.
[101] D. H. Ess, K. N. Houk, *J. Phys. Chem. A* **2005**, *109*, 9542–9553.
[102] S. Grimme, C. Mück-Lichtenfeld, E-U. Würthwein, A. W. Ehlers, T. P. M. Goumans, K. Lammertsma, *J. Phys. Chem. A* **2006**, *110*, 2583–2586. The B2-PLYP method adds a virtual orbital-dependent MP2 term to account for correct correlation energies.
[103] J. J. Blavins, P. B. Karadakov, D. L. Cooper *J. Org. Chem.* **2001**, *66*, 4285–4292.
[104] V. Branchadell, E. Muray, A. Oliva, R. M. Ortuño, C. Rodríguez-García, *J. Phys. Chem. A* **1998**, *102*, 10106–10112.
[105] a) C. Reichardt, *Solvents and Solvent Effects in Organic Chemistry*, VCH, Weinheim, **1990**; b) C.-J. Li, T.-K. Chan, *Organic Reactions in Aqueous Media*, Wiley, New York, **1997**.
[106] a) J. Sauer, R. Sustmann, *Angew. Chem. Int. Ed. Engl.* **1980**, *19*, 773; b) R. Huisgen, *Pure Appl. Chem.* **1980**, *52*, 2283.
[107] a) D. C. Rideout, R. Breslow, *J. Am. Chem. Soc.* **1980**, *102*, 7816; b) R. Breslow, U. Maitra, D. C. Rideout, *Tetrahedron Lett.* **1983**, *24*, 1901; c) R. Breslow, U. Maitra, *Tetrahedron Lett.* **1984**, *25*, 1239; d) R. Breslow, T. Guo, *J. Am. Chem. Soc.* **1988**, *110*, 5613; e) R. Breslow, C. J. Rizzo, *J. Am. Chem. Soc.* **1991**, *113*, 4340; f) R. Breslow, *Acc. Chem. Res.* **1991**, *24*, 159; g) R. Breslow, Z. N. Zhu, *J. Am. Chem. Soc.* **1995**, *117*, 9923.
[108] a) A. Rodgman, G. F. Wright, *J. Org. Chem.* **1953**, *18*, 465; b) T. R. Kelly, P. Meghani, V. S. Ekkundi, *Tetrahedron Lett.* **1990**, *31*, 3381.
[109] a) A. Meijer, S. Otto, J. B. F. N. Engberts, *J. Org. Chem.* **1998**, *63*, 8989; b) G. K. v. d. Wel, J. W. Wijnen, J. B. F. N. Engberts, *J. Org. Chem.***1996**, *61*, 9001; c) J. W. Wijnen, J. B. F. N. Engberts, *J. Org. Chem.* **1997**, *62*, 2039; d) K. E. Myers, K. Kumar, *J. Am. Chem. Soc.* **2000**, *122*, 12025.
[110] a) J. F. Blake, D. Lim, W. L. Jorgensen, *J. Org. Chem.* **1994**, *59*, 803; b) J. F. Blake, W. L. Jorgensen, *J. Am. Chem. Soc.* **1991**, *113*, 7430; c) W. L. Jorgensen, D. Lim, J. F. Blake, in: *Elementary Reaction in Heterogeneous Catalysis*, (Eds.: R. W. Joyner, R. A. van Santen), Kluwer, Dordrecht, **1993**, p. 377; d) D. Lim, C. Jenson, M. P. Repasky, W. L. Jorgensen, in: *Transition State Modeling for Catalysis*, (Eds.: D. G. Truhlar, K. Morokuma), ACS Symp. Ser. No. 721, American Chemical Society, Washington, DC, **1998**, Chapt. 6; e) W. L. Jorgensen, J. F. Blake, D. C. Lim, D. L. Severance, *J. Chem. Soc., Faraday Trans.* **1994**, *90*, 1727.
[111] J. Chandrasekhar, S. Shariffskul, W. L. Jorgensen, *J. Phys. Chem. B.* **2002**, *106*, 8078.
[112] a) R. N. Butler, A. G. Coyne, W. J. Cunningham, L. A. Burke, *J. Chem. Soc., Perkin Trans. 2* **2002**, 1807; b) R. N. Butler, W. J. Cunningham, A. G. Coyne, L. A. Burke, *J. Am. Chem. Soc.* **2004**, *126*, 11923.
[113] F.-G. Klärner, F. Wurche, *J. Prakt. Chem.* **2000**, *342*, 609.
[114] Y. Huang, V. H. Rawal, *J. Am. Chem. Soc.* **2002**, *124*, 9662.
[115] L. R. Domingo, J. Andrés, *J. Org. Chem.* **2003**, *68*, 8662.
[116] V. Polo, L. R. Domingo, J. Andrés, *J. Phys. Chem. A.* **2005**, *109*, 10438.
[117] For reviews see: a) P. L. Dalko, L. Moisan, *Angew. Chem. Int. Ed.* **2001**, *40*, 3726; b) P. L. Dalko, L. Moisan, *Angew. Chem. Int. Ed.* **2004**, *43*, 5138; c) K. N. Houk, B. List, (Eds.), *Acc. Chem. Res.* **2004**, *37*.
[118] W. Notz, F. Tanaka, C. F. Barbas III, *Acc. Chem. Res.* **2004**, *37*, 580.
[119] Y. Huang, A. K. Unni, A. N. Thadani, V. H. Rawal, *Nature* **2003**,*424*, 146.
[120] X. Zhang, H. Du, Z. Wang, Y.-D. Wu, K. Ding, *J. Org. Chem.* **2006**, *71*, 2862.
[121] a) F. Maseras, K. Morokuma, *J. Comput. Chem.* **1995**, *16*, 1170; b) M. Svensson, S. Humbel, R. D. J. Froese, T. Matsubara, S. Sieber, K. Morokuma, *J. Phys. Chem.* **1996**, *100*, 19357.
[122] K. A. Ahrendt, C. J. Borths, D. W. C. MacMillan, *J. Am. Chem. Soc.* **2000**, *122*, 4243.
[123] A. B. Northrup, D. W. C. MacMillan, *J. Am. Chem. Soc.* **2002**, *124*, 2458.
[124] a) W. S. Jen, J. J. M. Wiener, D. W. C. MacMillan, *J. Am. Chem. Soc.* **2000**, *122*, 9874; b) N. A. Paras, D. W. C. MacMillan, *J. Am. Chem. Soc.* **2001**, *123*, 4370; c) M. P. Brochu, S. P. Brown, D. W. C. MacMillan, *J. Am. Chem. Soc.* **2004**, *126*, 4108; d) J. F. Austin, D. W. C. MacMillan, *J. Am. Chem. Soc.* **2002**, *124*, 1172; e) N. A. Paras, D. W. C. MacMillan, *J. Am. Chem. Soc.* **2002**, *124*, 7894; f) S. P. Brown, N. C. Goodwin, D. W. C. MacMillan, *J. Am. Chem. Soc.* **2003**, *125*, 1192; g) J. F. Austin, S.-G. Kim, C. J. Sinz, W.-G. Xiao, D. W. C. MacMillan, *Proc. Natl. Acad. Sci. U. S. A.* **2004**, *101*, 5482; h) I. K. Mangion, A. B. Northrup, D. W. C. MacMillan, *Angew. Chem. Int. Ed.* **2004**, *43*, 6722.
[125] R. Gordillo, K. N. Houk, *J. Am. Chem. Soc.* **2006**, *128*, 3543.
[126] C. Allemann, R. Gordillo, F. R. Clemente, P. H.-Y. Cheong, K. N. Houk, *Acc. Chem. Res.* **2004**, *37*, 558.
[127] a) S. Bahmanyar, K. N. Houk, *J. Am. Chem. Soc.* **2001**, *123*, 11273; b) L. Hoang, S. Bahmanyar, K. N. Houk, B. List, *J. Am. Chem. Soc.* **2003**, *125*, 16; c) S. Bahmanyar, K. N. Houk, H. J. Martin, B. List, *J. Am. Chem. Soc.* **2003**, *125*, 2475; d) S. Bahmanyar, K. N. Houk, *Org. Lett.* **2003**, *5*, 1249; e) G. Wayner, K. N. Houk, Y. K. Sun, *J. Am. Chem. Soc.* **2004**, *126*, 199; f) T. Dudding, K. N. Houk, *Proc. Natl. Acad. Sci. U. S. A.* **2004**, *101*, 5770.
[128] a) H. C. Kolb, K. B. Sharpless, *Drug Discov. Today* **2003**, *8*, 1128; b) H. C. Kolb, M. G. Finn, K. B. Sharpless, *Angew. Chem. Int. Ed.* **2001**, *40*, 2004.
[129] a) R. Huisgen, H. Blaschke, *Chem. Ber.* **1965**, *98*, 2985; b) R. Huisgen, R. Knorr, L. Moebius, G. Szeimies, *Chem. Ber.* **1965**, *98*, 4014; c) R. Huisgen, H. Blaschke, *Liebigs Ann. Chem.* **1965**, *686*, 145; d) R. Huisgen, G. Szeimies, L. Moebius, *Chem. Ber.* **1967**,

100, 2494; e) R. Huisgen, G. Szeimies, L. Moebius, *Chem. Ber.* **1966**, *99*, 475; f) R. Huisgen, K. von Fraunberg, H. J. Sturm, *Tetrahedron Lett.* **1969**, 2589; R. Huisgen, *Pure Appl. Chem.* **1989**, *61*, 613.

[130] W. Lwowski, in: *1,3-Dipolar Cycloaddition Chemistry*, Vol. 1, (Ed.: A. Padwa), John Wiley & Sons, New York, **1984**, Chapter 5.

[131] a) V. V. Rostovtsev, L. G. Green, V. V. Fokin, K. B. Sharpless, *Angew. Chem. Int. Ed.* **2002**, *41*, 2596; b) H. C. Kolb, M. G. Finn, K. B. Sharpless, *Angew. Chem. Int. Ed.* **2001**, *40*, 2004.

[132] L. Zhang, X. Chen, P. Xue, H. H. Y. Sun, I. D. Williams, K. B. Sharpless, V. V. Fokin, G. Jia, *J. Am. Chem. Soc.* **2005**, *127*, 15998.

[133] A. Krasiński, V. V. Fokin, K. B. Sharpless, *Org. Lett.* **2004**, *6*, 1237.

[134] Z. P. Demko, K. B. Sharpless, *J. Org. Chem.* **2001**, *66*, 7945.

[135] F. Himo, Z. P. Demko, L. Noodleman, K. B. Sharpless, *J. Am. Chem. Soc.* **2002**, *124*, 12210, and references cited therein.

[136] For a treatise, see: *1,3-Dipolar Cycloaddition Chemistry*, Vols. 1 and 2, (Ed.: A. Padwa), John Wiley & Sons, New York, **1984**.

[137] F. Himo, Z. P. Demko, L. Noodleman, K. B. Sharpless, *J. Am. Chem. Soc.* **2003**, *125*, 9983.

[138] F. Himo, T. Lovell, R. Hilgraf, V. V. Rostovtsev, L. Noodleman, K. B. Sharpless, V. V. Fokin, *J. Am. Chem. Soc.* **2005**, *127*, 210.

[139] M. L. Kuznetsova, V. Yu. Kukushkin, *J. Org. Chem.* **2006**, *71*, 582.

